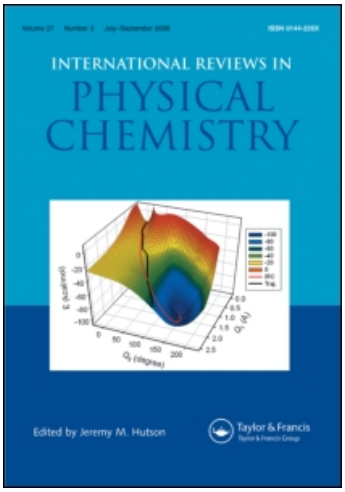

International Reviews in Physical Chemistry
Publication details, including instructions for authors and subscription information:
http://www.informaworld.com/smpp/title~content=t713724383

Periodic trends in the reactions of atomic ions with molecular hydrogen

P. B. Armentrout[a]
[a] Chemistry Department, University of Utah, Salt Lake City, Utah, USA

To cite this Article Armentrout, P. B.(1990) 'Periodic trends in the reactions of atomic ions with molecular hydrogen', International Reviews in Physical Chemistry, 9: 2, 115 — 148
To link to this Article: DOI: 10.1080/01442359009353244
URL: http://dx.doi.org/10.1080/01442359009353244

INTERNATIONAL REVIEWS IN PHYSICAL CHEMISTRY, 1990, VOL. 9, NO. 2, 115–148

Periodic trends in the reactions of atomic ions with molecular hydrogen

by P. B. ARMENTROUT
Chemistry Department, University of Utah,
Salt Lake City, Utah 84112, U.S.A.

One of the simplest possible reactions imaginable, that of an atomic ion with molecular hydrogen, shows a remarkable diversity in behaviour as the atomic ion is varied throughout the periodic table. Studies of these reactions reveal the fundamental changes that occur in the chemistry as the number of electrons is systematically varied. Here, we review our work on the kinetic energy dependence of these reactions as studied by using guided ion beam mass spectrometry. Substantial progress has been made in this area and now includes studies of 44 elements. This experimental technique is shown to provide unprecedented detail in reaction excitation functions over an extremely wide kinetic energy range. These studies allow an understanding of such effects as the reaction thermochemistry, electronic degeneracy, adiabatic *versus* diabatic potential energy surfaces and spin–orbit coupling.

1. Introduction

Opportunities to combine state-of-the-art chemical research with textbook examples of chemical principles seem few and far between these days. A candidate for such an opportunity is the systematic examination of the reactions of atomic ions with molecular hydrogen. These are among the simplest chemical reactions capable of addressing periodic trends in chemistry. Over the past two decades, the kinetic energy dependence of reaction (1) has been examined for many atomic ions, A^+. (In almost all

$$A^+ + H_2 \rightarrow AH^+ + H \tag{1}$$

circumstances, cross-sections for reaction of A^+ with D_2 are identical within experimental error to those for reaction with H_2. As a consequence, these systems may be used interchangeably in the discussions below.) Figure 1 shows the extent of progress made in this regard. Far from being a repetition of the same experiment, this set of studies varies wildly as one moves about the periodic table. These variations provide substantial insight into how the electron occupancy of atomic orbitals influences chemical dynamics. The intention of this review is to consolidate the results of these experiments and related studies of others by emphasizing this periodic nature.

Studies of reaction (1) are of interest for other diverse reasons. They include some of the simplest examples of ion–molecule reactions. Indeed, the reactions of $Ar^+ + H_2$ and $C^+ + H_2$ are often considered prototypical examples of exothermic and endothermic ion–molecule reactions. Some of these reactions (specifically, those of C^+, N^+, O^+, S^+, Cl^+) have been studied in detail due to their possible importance in interstellar chemistry, since H_2 is a major constituent of the interstellar medium (Watson 1977, Adams *et al.* 1984). Finally, the simplicity of these systems makes them amenable to detailed theoretical studies, both calculations of potential energy surfaces and detailed dynamic calculations. These provide insight which is not always evident from the experimental results.

0144-235X/90 $3·00

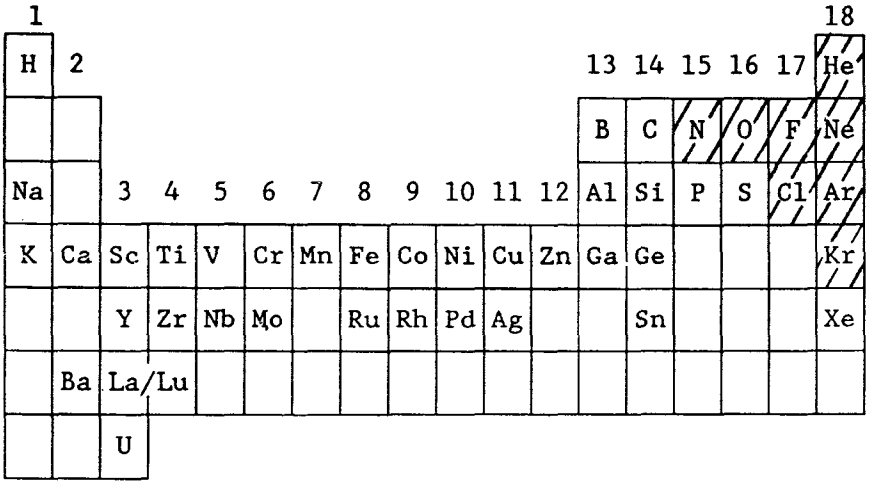

Figure 1. Periodic table showing those atomic ions A^+ for which reaction (1) has been studied as a function of kinetic energy. All but $A^+ = H^+$ and Ru^+ have been examined in our laboratory. Reaction (1) is exothermic or thermoneutral for those elements which are shaded.

Before our work, studies of the $A^+ + H_2$ reactions were largely restricted to those reactions that are exothermic. (Unless stated otherwise, thermochemical information is taken from the compilation of Lias *et al.* (1988).) This is simply because these reactions generally have large cross-sections and rate constants, and they are accessible to techniques designed to measure room-temperature rate constants (such as ion cyclotron resonance (ICR) mass spectrometry and flow tubes). As can be seen in figure 1, atomic ions which react exothermically include only a small subset of the periodic table. The vast majority of these reactions are endothermic and require beam techniques to be studied. A secondary emphasis of this review is therefore the dependence of these reactions on the kinetic energy of the reactants. This proves to be a very useful way of probing the potential energy surfaces of reaction systems, and thereby elucidating details of the kinetics, dynamics and thermodynamics of the systems (Armentrout 1988).

One relevant type of study which will not be discussed in detail here is the measurement of chemiluminescence from excited state products, as exemplified by the work of Ottinger and co-workers (Kusinoki and Ottinger 1979, 1980, 1982, 1984, Ottinger and Reichmuth 1981, Müller and Ottinger 1986a, b). While these can provide valuable insight into the dynamics of reaction (1), *absolute* cross-sections for production of the excited states cannot generally be derived. This means that the contribution to the total cross-section for reaction 1 cannot be ascertained. Further, studies in which the electronic state of the ion is poorly characterized will not be extensively included.

2. Experimental technique

Experiments in our laboratories are performed using a guided ion beam tandem mass spectrometer. This apparatus and the data reduction methods have been described in detail (Ervin and Armentrout 1985). Briefly, ions are formed in one of several available sources, extracted, and focused into a 60° magnetic sector for mass analysis. The mass-selected beam is decelerated to a desired kinetic energy (which can

vary from ~0·05 eV to over 500 eV) and focused into an octopole ion beam guide which passes through a collision cell containing the neutral reactant. Pressures of this gas are kept sufficiently low that single-collision conditions dominate. Product and reactant ions drift from the gas cell to the end of the octopole where they are extracted and focused into a quadrupole mass filter. After mass analysis, ions are detected using a secondary electron scintillation ion detector (Daly 1959) and counted using standard pulse counting electronics.

The octopole ion beam guide, first developed by Teloy and Gerlich (1974), is the primary key to the unique capabilities of this apparatus when compared with more conventional tandem mass spectrometers. This device uses r.f. fields to form a potential well in the radial direction, thus guiding ions along the instrumental axis. Energies along the axis of the octopole are perturbed very little and no consequences resulting from such a perturbation have been observed. The octopole potential well enables efficient collection of all products regardless of the reaction dynamics and routine determination of the absolute energy scale by using retarding techniques (Ervin and Armentrout 1985, Teloy and Gerlich 1974). The advantages of this when compared to conventional retarding field energy analysis have been described previously (Armentrout 1987).

Ion intensities are converted to absolute reaction cross-sections as described previously (Ervin and Armentrout 1985). Since our cross-section measurements are among the most precise every made, the accuracy of the cross-sections (with regard to both the absolute magnitude and absolute energy) has been ascertained by comparison with theoretical cross-sections and with thermal rate constants. These comparisons (see for example the discussion of the $O^+ + H_2$ system below) suggest that the accuracies of the cross-sections and energy scale are very good (uncertainties are generally less than 20% and 0·05 eV respectively).

Laboratory energies are converted to centre-of-mass (CM) energies using the stationary target assumption. Thus $E(\mathrm{CM}) = E(\mathrm{lab})m/(M+m)$ where m and M are the masses of the neutral and ionic reactants respectively. At the very lowest energies, this approximation is not adequate since the ion energy distribution is being truncated. The means of correcting for this has been discussed in detail (Ervin and Armentrout 1985). E(CM) does not include the thermal motion of the reactant neutral. These molecules have a Maxwell–Boltzmann distribution of velocities at 305 K, the gas cell temperature. The effects of this motion are particularly severe for reaction (1) (since H_2 is light) and obscure sharp features in the true excitation functions. This has been called Doppler broadening by Chantry (1971), and is explicitly accounted for in all quantitative analyses of our data (Ervin and Armentrout 1985).

Ion production is carefully controlled to generate specific states or a known distribution of states of the desired ion. Three types of ion sources are used most routinely in our experiments: surface ionization (Sunderlin and Armentrout 1988), electron impact (Elkind and Armentrout 1985) and high-pressure sources (Elkind and Armentrout 1986d). This versatility is possible because the ion source and reaction region are physically separated, in contrast to ICR and flow tube techniques. Selected-ion flow tube (SIFT) methods share this advantage to some degree, but here the state distribution of the ions is also influenced by interactions with the flow gas.

3. Theoretical

In order to understand the variations in the behaviour observed for reactions (1) as A^+ is varied, it will be useful to establish a theoretical background for these reactions.

This includes how ion–molecule reactions generally behave as a function of kinetic energy, the types of isotope effects that have been observed, and some simple molecular orbital concepts.

3.1. *Energy behaviour of ion–molecule reactions*

3.1.1. *Exothermic reactions*

The energy dependent cross-section for a reaction proceeding from reactants (channel 1) to products (channel 2) is $\sigma_{12}(E)$. Exothermic ion–molecule reactions are often (though not always) observed to proceed without an activation energy (Talrose *et al.* 1979) due to the attractive long-range potential induced by the charge. For molecules without permanent dipole moments (like H_2), σ_{12} is given fairly accurately by the Langevin–Gioumousis–Stevenson (LGS) equation (Gioumousis and Stevenson 1958),

$$\sigma_{LGS}=\sigma_{12}(E)=\pi e(2\alpha_1/E_1)^{1/2} \tag{2}$$

where e is the electron charge, α_1 is the polarizability of the neutral molecule in channel 1 (0·79 Å^3 for H_2, Hirshfelder *et al.* 1954), and E_1 is the relative kinetic energy of the species in channel 1. Deviations from this behaviour abound, as discussed by Henchman (1972) and Armentrout (1987), and as illustrated by the systems described below.

3.1.2. *Endothermic reactions*

For endothermic ion–molecule reactions, it might be expected that the energy behaviour can be predicted by microscopic reversibility as applied to equation (2) (Levine and Bernstein 1972). This yields the cross-section for proceeding from channel 2 to channel 1 as

$$\sigma_{21}(E)=\sigma_0(E_2-E_0)^{1/2}/E_2, \tag{3}$$

where E_0 is the endothermicity of the reaction, E_2 is the relative kinetic energy of the species in channel 2, and

$$\sigma_0=\pi e(2\alpha_1)^{1/2}(\mu_1 g_1/\mu_2 g_2) \tag{4}$$

where μ is the reduced mass of the species in the specified channel and g is the electronic degeneracy of the specified channel. While there are cases where equation (3) can accurately reflect the energy dependence of an endothermic ion–molecule reaction, experimentally this is rarely the case. However, equation (3) is also interesting as the only form of the cross-section for which the threshold energy, E_0, is identical to the Arrhenius 'activation energy'.

Alternate procedures for determining the threshold behaviour of ion–molecule reactions (or any reactions for that matter) include trajectory calculations, statistical theories, and empirical theories. Trajectory calculations potentially provide the most direct comparison between theory and experiment, but they are not generally useful because they require a very good potential energy surface, which is rarely available. More useful is the application of statistical theories such as phase-space theory (PST) or transition-state theory (TST). These theories require the molecular constants for all species in every reaction channel and, in the case of TST, for the intermediates as well. Dynamics are not explicitly included although conservation of angular momentum and energy are required. In our work, we have made extensive use of PST and found it to be fairly useful in describing the behaviour of several systems (Elkind and

Armentrout 1985, 1986a, 1986d, Ervin and Armentrout 1986b, 1987a, Weber *et al.* 1986). These comparisons make it clear that angular momentum effects are very important for bimolecular reactions. This has been emphasized by the work of Gerlich (Gerlich *et al.* 1987, Gerlich 1989b) who has also considered the role of nuclear spin.

The final method of describing the threshold behaviour of endothermic reactions is to develop empirical models of this behaviour. Such models can be quite general and are illustrated by equation (5),

$$\sigma_{21}(E)=\sigma_0(E_2-E_0)^n/E_2^m, \tag{5}$$

where σ_0 need not be given by equation (4) but is merely a scaling factor. Note that this form includes equation (3) as a particular example. Indeed, most theoretical predictions of the threshold behaviour can be expressed in this form (Aristov and Armentrout 1986). Unfortunately, for even the simple atom–diatom case, there are many theoretically predicted values of n and m, and experimentally, no one set of values for n and m works for all systems. Hence, in applying equation (5) to cross-section data, the values of σ_0, n, m and, if unknown, E_0, are treated as adjustable parameters. (Comparison to the data is made after the trial function is convoluted with the experimentally known ion and neutral energy distributions (Lifshitz *et al.* 1978.)) This procedure has proven to be quite adequate for reproducing the data very accurately over broad energy ranges. In most cases, the thermochemistry derived via E_0 compares favourably with any independent measures of the threshold energy. Exceptions to this latter statement can arise if there is an activation barrier in excess of the endothermicity. This is equivalent to there being a barrier to reaction in the exothermic direction. As discussed above, this is generally not true of ion–molecule reactions.

3.1.3. *Elevated kinetic energies*

At high kinetic energies, the consequences of energy disposal among the products need to be accounted for. In reaction (1), the excess energy available to the products must be in translation or in internal modes of AH^+. At sufficiently high reactant kinetic energies, the internal energy of AH^+ can exceed the dissociation energy of this diatom such that process (6) occurs.

$$A^+ + H_2 \rightarrow A^+ + H + H \tag{6}$$

This so-called indirect collision-induced dissociation has a thermodynamic threshold equal to $D^0(H_2)$, the bond energy of H_2 at 4·5 eV. As we shall see, cross-sections for formation of AH^+ in process (1) are often observed to decline rapidly above $D^0(H_2)$ due to the onset of process (6). This decline can be delayed in energy if the reaction dynamics tend to place much of the excess energy in product translation.

3.2. *Inter- and intra-molecular isotope effects*

One of the tools which we have used extensively in our studies of reaction (1) is examination of the inter- and intra-molecular isotope effects. In particular, the branching ratio between reactions (7 *a*) and (7 *b*),

$$A^+ + HD \rightarrow AH^+ + D, \tag{7a}$$

$$\rightarrow AD^+ + H, \tag{7b}$$

appears to be quite sensitive to the reaction dynamics. For endothermic reactions, three general classes of behaviour have been observed: 1, the branching ratio is near unity, 2,

process (7 *a*) is favoured by a factor of about three or four, and, 3, process (7 *b*) is favoured by a very large factor. Coupled with these observations are the fact that for classes 1 and 2 the reaction thresholds for H_2, HD and D_2 are all the same, given the differences in zero-point energy. This implies that the thermodynamic threshold is being observed. In contrast, for class 3, large shifts are observed in the thresholds for reactions (7 *a*) and (7 *b*) compared to those for reaction with H_2 and D_2. Clearly the thermodynamic thresholds are not observed here.

The first type of intramolecular isotope effect, class 1, is approximately the effect expected for a statistically behaved system (i.e. if all degrees of freedom are in equilibrium). This can be seen by examining the density of states for the products of reactions (7 *a*) *versus* (7 *b*). The following arguments presume that the mass of A greatly exceeds the mass of H and D, a reasonable approximation for all elements but H and He. The density of internal states favours production of AD^+. In the classical limit, the density of vibrational states is $1/\hbar\omega$. Since $\omega \propto 1/m^{1/2}$, where m is the reduced mass of the diatomic product ($m(AD^+) \approx 2$ and $m(AH^+) \approx 1$), this favours AD^+ by a factor of $2^{1/2}$. The classical density of rotational states is $1/hcB$ where $B \propto 1/m$ such that AD^+ is favoured by a factor of two. The density of translational states is proportional to $\mu^{3/2}$, where μ is the reduced mass of the reactant or product channel ($\mu(AD^+ + H) \approx 1$ while $\mu(AH^+ + D) \approx 2$). This favours AH^+ by a factor of $2^{3/2}$. Overall, these factors cancel such that the classical statistical isotope effect is about 1 : 1 formation of AH^+ and AD^+. This simple treatment ignores quantum effects but does capture the essence of a statistically behaved system. More detailed calculations using phase-space theory bear this out by giving a branching ratio near 1 : 1.

In class 2 behaviour, process (7 *a*) is observed to be favoured by a factor of three to four. Since it is the internal density of states that favours process (7 *b*) in the analysis above, the obvious means to enhance AH^+ production is to neglect this contribution. The internal and translational degrees of freedom no longer equilibrate and the reaction is no longer sensitive to the density of internal energy states. In other words, the reaction is direct. This favours production of AH^+ by a factor of $2^{3/2} = 2{\cdot}8$. We have previously pointed out that an equivalent way of thinking about this effect is in terms of angular momentum conservation (Elkind and Armentrout 1985, Aristov and Armentrout 1986, Sunderlin *et al.* 1987). This analysis also concludes that the reaction must be direct.

Class 3 behaviour is an unusual effect but not an uncommon one for reaction (1). This arises when the potential energy surface for reaction is repulsive. This leads to a hard-sphere or *impulsive* type of reaction in which the dominant interaction is a 'pairwise' one between A^+ and closest atom of H_2, D_2 or HD. This means that the energy relevant to reactions (1) and (7) is not the centre-of-mass (CM) energy but a pairwise interaction energy. In the CM system, the energy available to cause chemical change is the relative kinetic energy between the incoming atom (having mass A) and the reactant molecule BC (having mass $B+C$). Hence

$$E(\mathrm{CM}) = E(\mathrm{lab})(B+C)/(A+B+C),$$

where E(lab) is the energy of the ion in the laboratory frame. In a pairwise interaction, A is sensitive only to the potential between A and the atom B which is transferred in reactions (1) and (7). Hence the pairwise energy for transfer of B from molecule BC is

$$E(\mathrm{pair}) = \frac{E(\mathrm{lab})B}{A+B} = \frac{E(\mathrm{CM})(A+B+C)B}{(B+C)(A+B)}.$$

This shows that the energy available for chemical change in the pairwise frame is *always* less than in the CM frame. This is most easily seen for situations (like reactions (1) and (7)) where $A \gg B$ or C. Then, E(pair) is approximately $E(\mathrm{CM})B/(B+C)$. For reaction where $BC = H_2$ or D_2, the factor $B/(B+C)$ is $\frac{1}{2}$; while for $BC = HD$, it is $\frac{1}{3}$; and for $BC = DH$, it is $\frac{2}{3}$. This means that for a reaction which is endothermic by E_0, the pairwise threshold will occur at a CM energy of $2E_0$ in reaction with H_2 or D_2; at $3E_0$ for reaction (7 *a*); and at $1{\cdot}5E_0$ for reaction (7 *b*). This pairwise scheme readily explains the shifts in threshold observed for the H_2, HD and D_2 systems, and suggests that the enhanced production of AD^+ in process (7 *b*) is due to the lower apparent threshold for this reaction compared to that for reaction (7 *a*). This extraordinary effect will become evident in the examples given below.

It should be noted that this pairwise energy frame may be familiar from the 'spectator stripping' model (SSM) (Henglein 1966). The SSM is a highly specific example of a model which incorporates the pairwise energy concept. The difference is that the SSM allows no momentum transfer to the product atom C while the more general pairwise model does not forbid such a transfer. Thus the SSM makes a very specific prediction about the velocity and internal energy of the products while the pairwise model allows for distributions of these quantities. The latter, not surprisingly, corresponds most readily to observation. The point of the exercise above is that the pairwise energy scale, an extremely useful concept, can easily be derived without the severe assumption made in the SSM.

3.3. *Molecular orbital considerations*

A great deal of insight into reaction (1) can be obtained by using simple molecular orbital (MO) arguments (Mahan 1971, 1975, Elkind and Armentrout 1985, Armentrout 1987).

3.3.1. s *orbitals*

Consider first the interaction of an s orbital on the atomic ion A^+ with a hydrogen molecule in C_{2v} symmetry (perpendicular approach). Since the $s(A^+)$ and $\sigma_g(H_2)$ orbitals both have a_1 symmetry, they mix to form bonding and antibonding MOs. The two electrons which start in the $\sigma_g(H_2)$ orbital occupy the bonding a_1 MO. Thus, occupation of the $s(A^+)$ leads to occupation of the antibonding a_1* MO. This leads to a repulsive interaction between A^+ and H_2 which is not present if the $s(A^+)$ orbital is empty. Since the $\sigma_u(H_2)$ orbital has b_2 symmetry, it does not interact with the $s(A^+)$ orbital in C_{2v} symmetry.

In $C_{\infty v}$ symmetry (collinear approach), the situation changes somewhat. Now the $s(A^+)$ orbital interacts with both $\sigma_g(H_2)$ and $\sigma_u(H_2)$ such that three MOs are formed: one is bonding, another is largely non-bonding, and the third is antibonding. The two electrons in the $\sigma_g(H_2)$ orbital again go into the bonding MO. Occupation of $s(A^+)$ therefore leads to occupation of the non-bonding MO. This results in an interaction which is less repulsive than that resulting from occupation of the antibonding a_1* MO in C_{2v} symmetry but is still less attractive than if the $s(A^+)$ orbital (and hence the non-bonding MO) were empty.

Classic examples of these ideas are the reactions of $H^+ + H_2$ and $H + H_2$. In the former system, the $s(H^+)$ orbital is empty such that the reaction occurs preferentially via the C_{2v} geometry. This leads to the triangular ground state of the H_3^+ intermediate.

In the $H+H_2$ system, the s(H) orbital is singly occupied and hence the C_{2v} geometry approach is highly repulsive. This leads to a collinear ($C_{\infty v}$) interaction as the preferred reaction pathway, but one which retains a barrier to reaction.

3.3.2. p *orbitals*

Extension of these ideas to p orbitals on the atomic ion are straightforward. In C_{2v} symmetry (where the atom approaches along the z axis and the x–z plane is defined by the three atoms), the $p_z(A^+)$ orbital (having a_1 symmetry) behaves the same as the $s(A^+)$ orbital, described above. The $p_y(A^+)$ orbital is out of the plane of the three reactant atoms and therefore has no interaction with H_2. The new consideration is that the $p_x(A^+)$ orbital can interact with $\sigma_u(H_2)$ since both have b_2 symmetry. These combine into bonding and antibonding MOs but since $\sigma_u(H_2)$ is empty, occupation of the $p_x(A^+)$ orbital leads to occupation of the bonding $b_2(AH_2^+)$ MO. This leads to an attractive bonding interaction between A^+ and H_2. In $C_{\infty v}$ symmetry, both the $p_x(A^+)$ and $p_y(A^+)$ are non-bonding and the $p_z(A^+)$ orbital again behaves as described above for the $s(A^+)$ orbital. The consequences of these ideas now depend on the specific occupations of the orbitals on the reactant atom. These will be discussed for individual cases below.

3.3.3. d *orbitals*

Extension of these concepts to d orbitals has enabled a detailed understanding of the state-specific reactivity of atomic transition metal ions with H_2 (Elkind and Armentrout 1985, 1987b). Much like the p orbitals, the interaction of the d orbitals with H_2 can be separated into three types: (1) the $d\sigma(z^2)$ which like the p_z interacts strongly with H_2 in both C_{2v} and $C_{\infty v}$ symmetries; (2) the $d\pi(xz)$ which like the p_x interacts in only C_{2v} geometry; and (3) the $d\pi(yz)$, $d\delta(xy)$ and $d\delta(x^2-y^2)$ which like the p_y are largely non-bonding. However, to understand the interactions of atomic transition metal ions with H_2, it must be realized that an s orbital is the outermost valence orbital on these metal ions as well as a principal binding orbital in the diatomic metal hydride ions. Thus the interaction of this orbital (rather than the d orbitals) with H_2 is expected to be dominant at long range. The interactions of the d orbitals with H_2 are important when the valence s orbital is empty. These ideas have been detailed elsewhere (Elkind and Armentrout 1987b, Armentrout 1989, 1990).

3.3.4. *Adiabatic, diabatic and non-adiabatic*

Several terms which will be used extensively in the following discussion are adiabatic, diabatic and non-adiabatic. In this paper, we use the term diabatic to refer to a potential energy surface (PES) which evolves from reactants to products with an unchanged electron configuration (atomic orbital population). Diabatic PESs can and often do cross one another. If such surfaces have the same spin and the same orbital symmetry, then the crossing is avoided and the surfaces combine to form two new adiabatic PESs. Under ordinary conditions at thermal energies, reactive systems generally evolve along adiabatic surfaces. At high kinetic energies, nuclear motion may be rapid enough that electrons do not relax to the lowest energy surface. Thus the system behaves diabatically. This is one type of non-adiabatic effect. Spin–orbit mixing and other effects may also induce non-adiabatic behaviour in a reacting system.

4. Group 1: hydrogen and alkali metals

Ions of the group 1 elements have no valence electrons. Their inert-gas-like electron configurations mean they are exceptionally stable and unreactive. Their interaction with H_2 should be dominated by donation of the $\sigma_g(H_2)$ electrons to the empty s(A^+) orbital.

4.1. *Hydrogen*

This is the unique member of this periodic column due to the identity of the three nuclei in reaction (1) where $A^+ = H^+$. As a consequence, reaction (1) has been examined only by isotope substitution studies. Furthermore, reaction (1) (which is equivalent to the charge transfer process) is endothermic by 1·83 eV and cannot be studied at thermal energies. At these low energies, pertinent studies include the work of Henchman *et al.* (1981) where the selected-ion flow tube (SIFT) technique was used to measure the forward and reverse rates of reactions (8) and (9) as a function of temperature:

$$H^+ + D_2 \leftrightarrow D^+ + HD, \tag{8}$$

$$D^+ + H_2 \leftrightarrow H^+ + HD. \tag{9}$$

Good agreement with theoretical values based on zero-point energy differences and statistical factors was found. Consistent results were also found for these reactions at higher kinetic energies by Villiger *et al.* (1982) in a flow-drift measurement.

At still higher kinetic energies, where reaction (1) can be observed, the most definitive study is one of the early applications of guided-ion-beam technology. Ochs and Teloy (1974) studied the interaction of H^+ with D_2 and determined the cross-sections for all four possible reaction channels: $D^+ + HD$, $D^+ + H + D$, $HD^+ + D$ and $D_2^+ + H$. These results were found to be in excellent agreement with trajectory surface hopping calculations of Krenos *et al.* (1974), although not with the experimental results of these authors. Another impressive result is the partial resolution of rotational excitation in reaction (8) reported by Gerlich (1989a).

4.2. *Alkali metals*

Our attempts to look for reaction (1) with $A^+ = Na^+$ and K^+ have revealed no reactivity (J. L. Elkind and P. B. Armentrout 1986, unpublished work). This is consistent with what little is known about the thermochemistry of the alkali-hydride ions. Heats of formation compiled by Lias *et al.* (1988) can be used to calculate bond energies for Li^+–H of 3 kcal mol^{-1} and for K^+–H of -40 ± 23 kcal mol^{-1}. While the latter result is clearly absurd, the binding of the alkali-hydride ions is clearly very weak.

While reaction (1) has not been observed for alkali ions, inelastic scattering of these ions with hydrogen has been studied extensively. For the purposes of this review, the conclusions of Dimpfl and Mahan (1974) are the most pertinent. They found that the primary interaction between Na^+ and D_2 occurred in a perpendicular geometry rather than a collinear one. Since the Na^+(3s) orbital is empty, this would be the prediction of the molecular orbital ideas discussed above.

5. Group 2: alkaline earth metals

The alkaline earth metal ions have only a single electron in the valence s orbital. The molecular orbital ideas discussed above suggest that this should lead to a collinear reaction geometry (like $H + H_2$). Potential energy surfaces have been calculated for the simplest of these systems, $Be^+ + H_2$ (Raimondi and Gerratt 1983), although these were

restricted to include only collinear geometries and sigma states of BeH^+. This work finds a shallow potential well for Be^+–H–H (0·05 eV) and a small barrier of 0·07 eV in excess of the endothermicity. The simplest system, $Be^+ + H_2$, has yet to be studied experimentally; but experiments involving calcium and barium ions have been performed.

5.1. *Calcium*

We recently examined the reaction of Ca^+ with H_2, HD, and D_2 for the first time (Georgiadis and Armentrout 1988). Results for the HD system are shown in figure 2 (*a*). These cross-sections and those for the H_2 and D_2 systems rise rapidly from thresholds consistent with the rough thermochemistry known. The cross-section can be interpreted by using equation (5) or phase space theory (PST). These measurements provide the 0 K bond energy, $D_0^0(Ca^+–H) = 1{\cdot}97 \pm 0{\cdot}12$ eV. While PST accurately models the shape of the cross-section for reaction (1), it cannot reproduce its absolute magnitude (the experimental results are a factor of 20 smaller) nor the branching ratio for reactions (7 *a*) and (7 *b*). This branching ratio (which favours reaction (7 *a*) by a factor of four) is a nice example of the second type of intramolecular isotope effect discussed above, that for direct reactions.

The direct nature of this reaction is explained by the molecular orbital arguments which predict a preference for collinear reaction geometry. This means that a long-lived

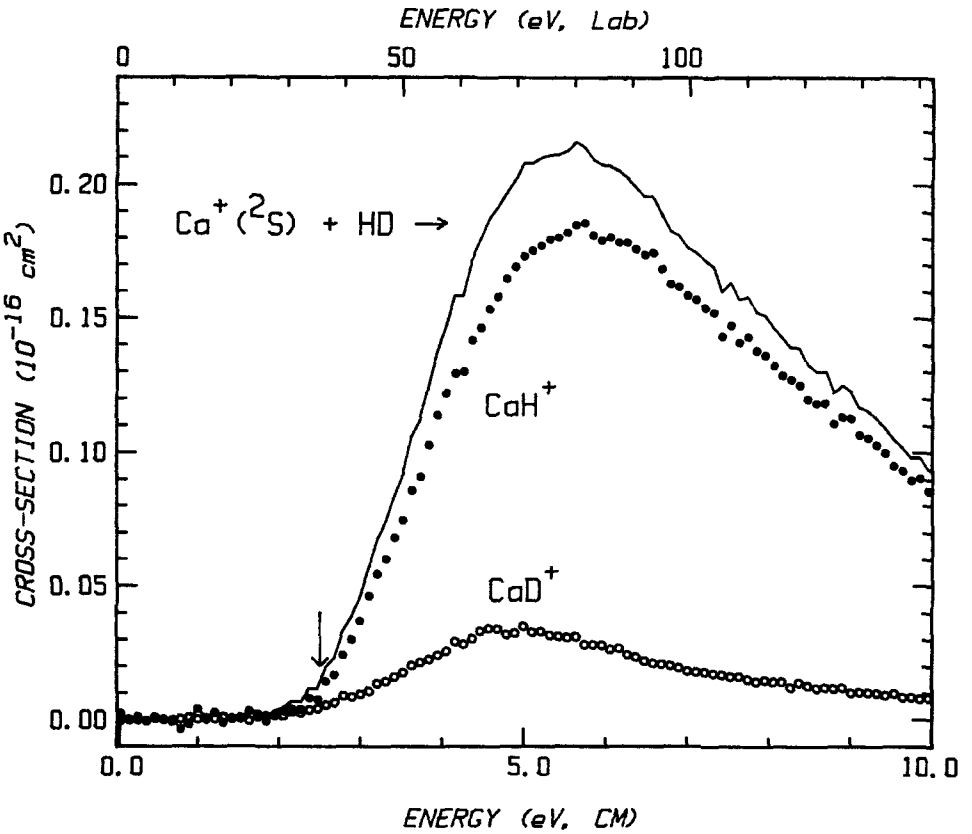

(*a*)

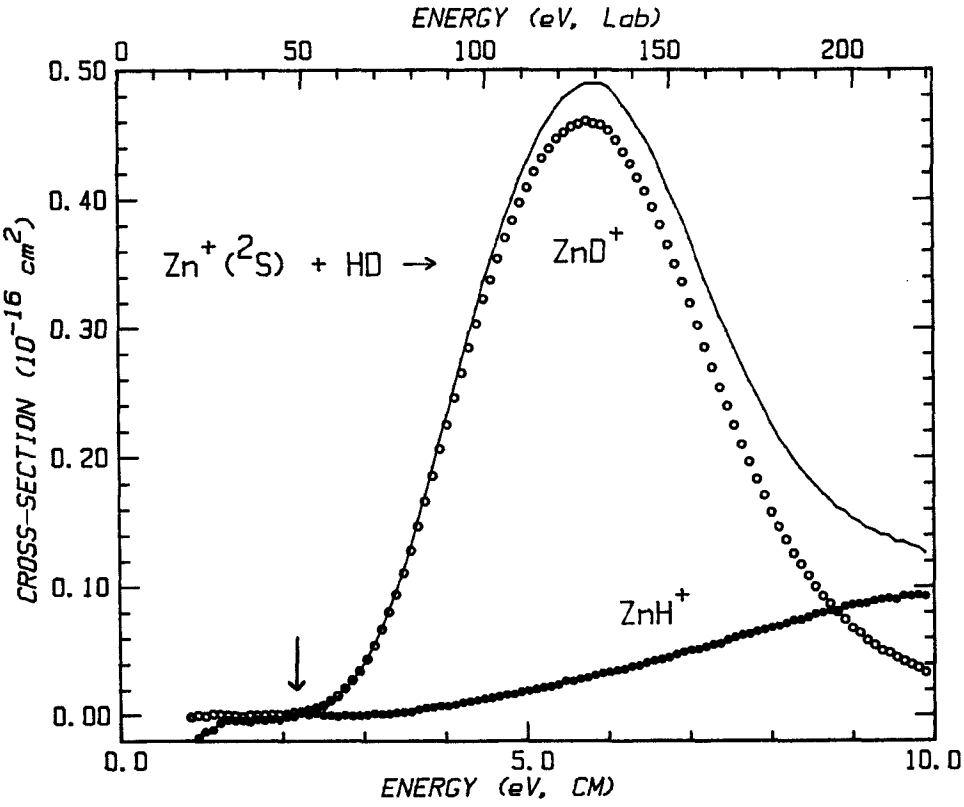

(*b*)

Figure 2. Cross-sections for reactions (7 *a*) and (7 *b*) for $A^+ = Ca^+(^2S)$ (*a*) and $A^+ = Zn^+(^2S)$ (*b*) as a function of kinetic energy in the centre-of-mass frame (lower scale) and laboratory frame (upper scale). The arrows show the thermodynamic thresholds for reaction.

CaH_2^+ intermediate is not easily formed, and thus the reaction cannot exhibit statistical behaviour. The restriction to near-collinear collisions can also explain why the cross-section is small.

5.2. *Barium*

The Ba^+ study was an early ion-beam experiment (Armentrout and Beauchamp 1980a) in which only the D_2 reaction was examined. Formation of BaD^+ was found to be endothermic by 2·1 eV, leading to a bond energy of $D^0(Ba^+–D) = 2{\cdot}5 \pm 0{\cdot}1$ eV. The energy dependence of the cross-section was interpreted by using an extension of the sequential impulse model (SIM) for direct reactions (Mahan *et al.* 1976). Good agreement was found throughout the energy range studied, 0–10 eV. The utility of a model for direct reactions is consistent with the prediction of the molecular orbital picture (although it might be noted that this model does not enjoy similar success for reaction (1) with Ca^+).

6. Groups 3–11: transition metals

One of the intimidating features of the study of transition metal ions is the large number of electronic states. For instance, Ti^+ has eight electronic states below 1·5 eV

(22 spin–orbit levels) which can form 128 separate potential energy surfaces in the interaction with H_2. Clearly, explicit accounts of all these surfaces cannot be achieved easily. Our recent work on these systems was directed at addressing whether any account of the influence of electronic states could be achieved. Are there simple unifying features which govern transition metal reactions? If we cannot evaluate the influence of excited states in the simplest imaginable reaction, process (1), there would seem to be little hope of doing so in more complex (and chemically interesting) systems.

6.1. *First-row transition metals*

The earliest studies of reaction (1) where A^+ is a transition metal ion were performed by Armentrout and Beauchamp (1980b, 1980c, 1981). More recently, Elkind and Armentrout (1985, 1986a, 1986c, 1986d, 1986e, 1987a, 1988) and Elkind *et al.* (1989) have performed detailed studies of the reactions of all the first-row transition metal ions with H_2, HD and D_2. A distinguishing feature of this work is that particular attention is paid to the effects of electronic excitation. This work has been reviewed elsewhere (Elkind and Armentrout 1987b, Armentrout 1987, 1989), but an example of the type of behaviour which can occur is shown in figure 3. The ground state $Fe^+(^6D, 4s3d^6)$ reacts

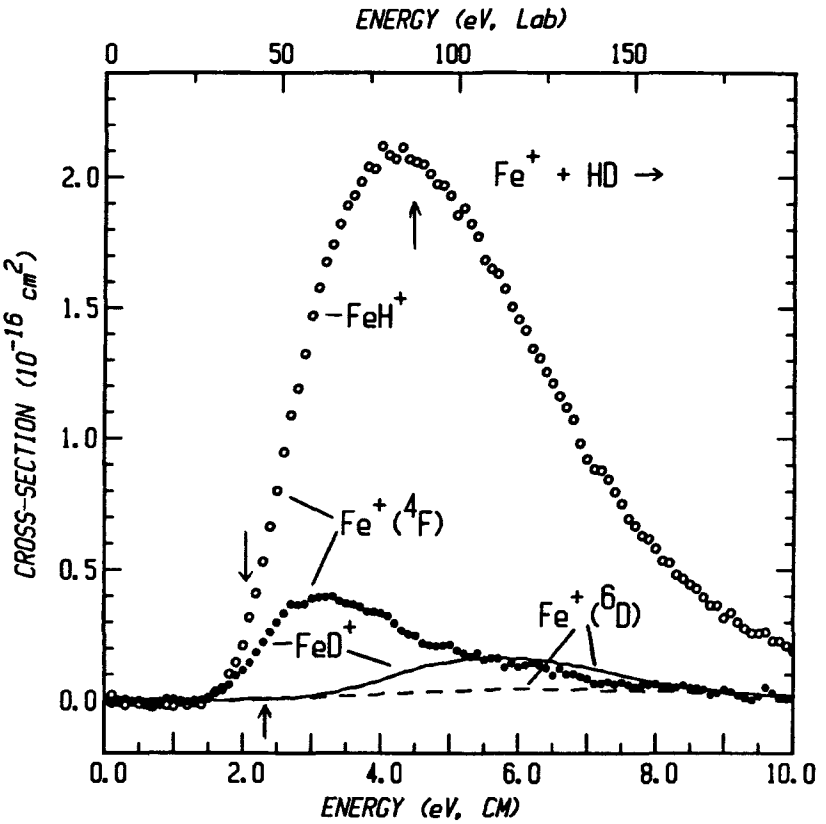

Figure 3. Cross-sections for reactions (7 *a*) (open circles and dashed line) and (7 *b*) (closed circles and full line) for $A^+ = Fe^+(^4F)$ and $Fe^+(^6D)$ as a function of kinetic energy in the centre-of-mass frame (lower scale) and laboratory frame (upper scale). Arrows indicate the thresholds for reaction of $Fe^+(^4F)$ and $Fe^+(^6D)$ at 2·1 and 2·4 eV respectively, and the bond energy of HD at 4·55 eV.

inefficiently with an elevated threshold and produces much more FeD^+ than FeH^+ (impulsive behaviour). In contrast, the first excited state $Fe^+(^4F, 3d^7)$ which is only 0·25 eV higher in energy reacts readily at the thermodynamic threshold and produces about three times more FeH^+ than FeD^+ (a direct reaction).

These behaviours are representative of other metal ions having similar electron configurations, $4s3d^{n-1}$ (where the 4s electron is high-spin coupled to the 3d electrons) and $3d^n$ ($n>5$) respectively. Metals that have configurations $4s3d^{n-1}$ (where the 4s electron is low-spin coupled to the 3d electrons) behave similarly to $Fe^+(^4F)$. Metal ions with $3d^n$ ($n<5$) configurations show distinct behaviour. For these metal ions, the branching ratio in reaction with HD is nearly 1 : 1 indicating statistical behaviour.

In these cases, the results can be easily interpreted by using the MO concepts outlined above. For some metal ions, however, there are variations in the expected behaviour which can be attributed to the interaction of different potential energy surfaces (i.e. the diabetic reactivity is no longer followed because the reaction follows adiabatic surfaces which mix the electron configuration character).

6.2. *Second-row transition metals*

The only detailed studies of the reactions of second row transition metal ions with hydrogen which have been published concern Y^+ (Elkind *et al.* 1989), Ru^+, Rh^+ and Pd^+ (Mandich *et al.* 1984). For the latter three, the work was directed primarily at determining the thermochemistry of the AH^+ bond, so no studies with HD were performed. While the detailed results have yet to be published, we have studied most of the second-row transition metal ion reactions (all but Tc^+ and Ru^+) and reported the thermochemical results (Elkind and Armentrout 1986b, Armentrout and Georgiadis 1988, Armentrout and Beauchamp 1989). In the cases where results for HD have been obtained, our studies indicate that there are both similarities (Y^+ and Sc^+ both react via insertion, Rh^+ and Co^+ both react by direct processes) and differences (Mo^+ shows distinct behaviour from Cr^+) with the first-row analogues.

6.3. *Third-row transition metals, lanthanides and actinides*

Of these elements, studies of reaction (1) have been made with only three, namely La^+, Lu^+ and U^+. Our recent work concerning the former two elements (Elkind *et al.* 1989) concentrated on examining the periodic trends as one moved down a column of the periodic table. While Sc^+, Y^+, and La^+ all reacted with H_2, HD and D_2 similarly, Lu^+ exhibited very different behaviour. While all four metal ions have two valence electrons, this result can be rationalized by the electronic configurations of these metals. Sc^+, Y^+ and La^+ all have low-lying states with a d^2 valence configuration which the MO ideas find is quite reactive. Such a state for Lu^+ is very high in energy (because of the fully occupied 4f shell). Instead, ground state $Lu^+(^1S, 6s^2)$ has the valence 6s orbital fully occupied. This leads to a strong repulsion in the interaction of Lu^+ with H_2.

One of the earliest studies of the interactions of a metal ion with H_2 concerned the reaction of U^+ with D_2 (Armentrout *et al.* 1977a, 1977b). The emphasis here was on a derivation of the bond energy, $D^0(U^+–D) = 2·9 \pm 0·1$ eV. The quality of the data and its interpretation are fairly crude.

7. Group 12: zinc

Zinc is the only group 12 element for which reaction (1) has been examined. This work was coupled with our study of reaction (1) for Ca^+ (Georgiadis and Armentrout 1988). Our interest here was to see what influence occupation of the 3d orbitals might

have on this reaction. Both atomic ions have a single electron in the 4s orbital, and in Ca^+ the 3d orbitals are empty, while in Zn^+, they are fully occupied. The results for the $Zn^+ + HD$ system are compared with those for Ca^+ in figure 2. The Zn^+ cross-sections shown and those for the H_2 and D_2 systems rise slowly from thresholds which vary from reaction to reaction. The shape of the cross-section cannot be interpreted by using phase space theory, although equation (5) can roughly reproduce the cross-sections (but with very different values of n compared to those for Ca^+). This branching ratio is a nice example of the third type of intramolecular isotope effect discussed above, that for impulsive reactions.

The difference in behaviour of the Ca^+ and Zn^+ systems demonstrates some of the subtleties of reaction (1). Since the outermost valence orbital occupation is the same for both of these ions, the dominant interactions with hydrogen should be similar. The fact that they are not can be explained by examining the participation of the 3d orbitals. In the Ca^+ system, these empty orbitals lie somewhat above the 4s orbital energy. As for a $p_x(b_2)$ orbital, interaction of the $3d\pi(b_2)$ orbital is favourable and crosses the orbital evolving from the $4s(a_1)$ orbital. By allowing these orbitals to mix (in C_s symmetry), the repulsiveness of the potential energy surface is mediated in the case of Ca^+ for non-collinear geometries. In essence, the repulsion is removed by allowing the 4s electron to migrate to the bonding $3d\pi(b_2)$ orbital. No such favourable interaction occurs in the case of Zn^+ because the 3d orbitals are fully occupied and much too low in energy to participate. Thus reaction is largely restricted to a repulsive collinear reaction geometry, resulting in the impulsive type of interaction.

8. Group 13: boron, aluminium and gallium

With their $(ns)^2(np)^0$ ground state electron configuration, the group 13 elements have the distinction of having both filled and empty valence orbitals. One might therefore anticipate that the interaction with H_2 would be dominated by the repulsion with the occupied s orbital, but the possibility of moving electrons into the empty p orbital could result in a much more attractive surface. Experimentally, this is one of the more poorly characterized groups of the periodic table. Results for reaction (1) have been reported only for boron, and there appears to be some discrepancies. We have preliminary results for this element as well as aluminium and gallium (J. L. Elkind and P. B. Armentrout 1986, unpublished work).

8.1. *Boron*

In the first report of reaction (1) with $A^+ = B^+$, Lin *et al.* (1974b) found that the ^3P excited state of B^+ reacts with D_2 efficiently in an exothermic process while the ^1S ground state reaction is endothermic. Further work by this group (Sondergaard *et al.* 1979, 1982) showed that the ground state reacted via a persistent complex to form both the $X^2\Sigma^+$ and the $A^2\Pi$ state of the BD^+ product. The excited state was found to undergo the exothermic formation of $BD^+(X^2\Sigma^+)$ via a complex, and the endothermic formation of $BD^+(A^2\Pi)$ via a direct reaction. This contrasts with the work of Friedrich and Herman (1982), who concluded that the formation of the $A^2\Pi$ state from $B^+(^3P)$ also occurs via a long-lived intermediate. For excited state reactants, formation of excited products has been confirmed by the chemiluminescence studies of Ottinger and Reichmuth (1981). While no quantitative estimates are made of the extent of $X^2\Sigma^+$ *versus* $A^2\Pi$ state formation, all these results seem to suggest that the extent of excited state formation is appreciable.

In the study of Lin *et al.* (1974b), the cross-section for reaction of $B^+(^1S)$ was observed to rise rapidly from an energy near the expected threshold of about 2·5 eV and to peak near the threshold for reaction (6). This result contrasts with the more recent observations of Ruatta *et al.* (1989) who found a cross-section which rises slowly from a threshold pushed to higher energies and peaked near 8 eV. This latter observation is in reasonable agreement with the data shown in figure 4 (J. L. Elkind and P. B. Armentrout 1986, unpublished work). Included in this preliminary study are results for the interaction of $B^+(^1S)$ with HD, figure 5. While more refined results are needed for a definitive analysis, the isotope effect observed here is quite unusual but conforms most closely to the impulsive type of result discussed above. This suggests a strongly repulsive surface for reaction which appears to be inconsistent with the formation of a long-lived complex.

There are several interesting features of the ground state reaction system which require explanation. This is facilitated by the extensive theoretical work which this system has seen (Hirst 1983, Schneider *et al.* 1984a, 1984b, Rosmus and Klein 1984, Cooper *et al.* 1986, Klimo *et al.* 1986). As noted by Sondergaard *et al.* (1982), the interaction of $B^+(^1S)+H_2(^1\Sigma_g^+)$ should be repulsive but can form the strongly bound $H\text{–}B^+\text{–}H(^1\Sigma_g^+)$ intermediate via an adiabatic crossing with the surface evolving from $B^+(^1P)$, which has a 2s2p electron configuration. *Ab initio* calculations by Rosmus and Klein (1984) show that the lowest-energy pathway for this process is tortuous: $B^+(^1S)$

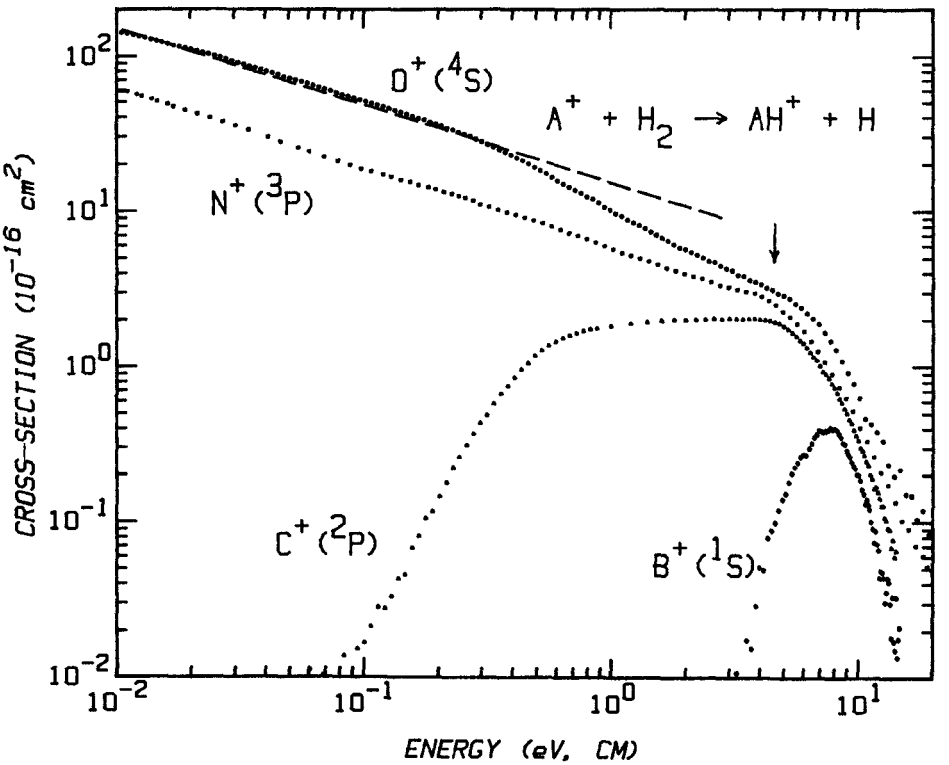

Figure 4. Cross-sections for reaction (1) for $A^+=B^+(^1S)$, $C^+(^2P)$, $N^+(^3P)$ and $O^+(^4S)$ as a function of kinetic energy in the centre-of-mass frame. The dashed line is σ_{LGS}, calculated by using equation (2). The arrow marks the bond energy of H_2 at 4·5 eV.

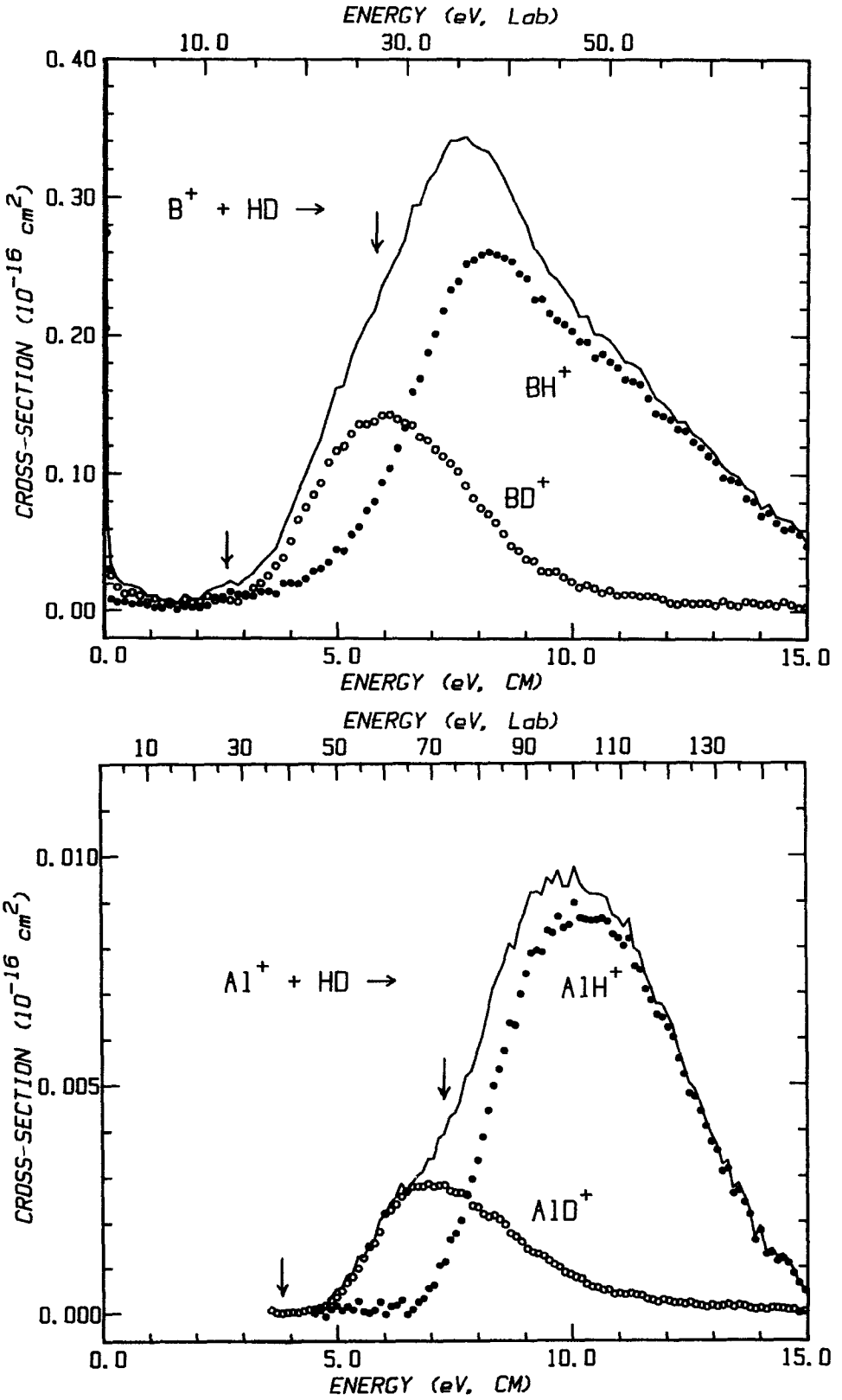

Figure 5. Cross-sections for reactions (7 *a*) and (7 *b*) for $A^+ = B^+(^1S)$ (*a*) and $A^+ = Al^+(^1S)$ (*b*) as a function of kinetic energy in the centre-of-mass frame (lower scale) and laboratory frame (upper scale). Arrows indicate the thermodynamic thresholds for formation of the $X^2\Sigma^+$ and $A^2\Pi$ states of the products.

approaches H_2 with a collinear geometry (to minimize repulsive interactions) and then twists around to insert into the H_2 bond at closer distances. These calculations find that this pathway has a barrier which is comparable to the endothermicity of the overall reaction to form $BH^+(X^2\Sigma^+)$. Since it is unlikely that this lowest-energy pathway can be followed for reactants with kinetic energies of 2·5 eV and higher, this could explain the observation of inefficient reactivity at threshold in our laboratories and by Ruatta *et al.* (1989), and seems inconsistent with the cross-section observed by Lin *et al.* (1974b).

Formation of $BH^+(A^2\Pi)+H(^2S)$ from $B^+(^1S)+H_2(^1\Sigma_g^+)$ is also intriguing since there is no adiabatic pathway for this reaction, as noted by Sondergaard *et al.* (1982). These authors suggest that this reaction occurs by coupling the $^1A_1$ reactant surface (in C_s symmetry) with the $^3B_1$ surface evolving from $B^+(^3P)$ while Hirst (1983) and Rosmus and Klein (1984) suggest coupling to the $^1B_2$ surface evolving from $B^+(^1P)+H_2$. Since no spin flip is required in the latter mechanism, it is probably more reasonable, but, in either case, it is clear that the B^+ reactant needs to build $(2s)^1(2p)^1$ character into the ground state $(2s)^2$ configuration. This is consistent with the qualitative molecular orbital ideas.

8.2. *Aluminium*

The only published experimental work for reaction (1) is the chemiluminescence studies of Müller and Ottinger (1986a). These authors find that the results parallel those for the boron system although a large activation barrier of ~3·5 eV is found for formation of $AlH^+(A^2\Pi)$ from excited state $Al^+(^3P)$. The theoretical work of Hirst (1987) finds that the $AlH_2^+(^1\Sigma_g^+)$ intermediate is metastable with respect to reactants (in contrast to the case for boron) and that there is no barrier to formation of $AlH^+(X^2\Sigma^+)$ in excess of the endothermicity for a collinear reaction geometry. Formation of $AlH^+(A^2\Pi)$ can occur via a mechanism similar to that suggested for $BH^+(A^2\Pi)$.

Preliminary work in our laboratories yields a result which is quite different. As shown in figure 6, reaction (1) is very inefficient (the maximum cross-section does not exceed 10^{-18} cm^2) and is not observed until an apparent threshold of 6·5 eV, well over the thermodynamic threshold of ~3·8 eV. The cross-section peaks at about 9 eV. Reactions (7 *a*) and (7 *b*) have cross-sections which behave much like those for boron (figure 5). While these results await detailed analysis, it is clear that this system is behaving impulsively and that a considerable barrier to reaction is present. This is in agreement with the observations of Müller and Ottinger (1986a).

8.3. *Gallium*

Preliminary work in our laboratories has examined the reaction of Ga^+ with D_2. We find that the cross-section behaves similarly to that for Al^+. It has an apparent threshold of about 9 eV and reaches a maximum of only 4×10^{-20} cm^2 at ~10·5 eV.

9. Group 14: carbon, silicon, germanium and tin

The group 14 ions have three valence electrons with a configuration $(ns)^2(np)^1$. The interaction with hydrogen is dominated by the lone p electron. If this electron resides in the p_x orbital, an attractive surface ($^2B_2$ in C_{2v} or $^2\Pi$ in $C_{\infty v}$) results. If the p_z is occupied, a repulsive surface of $^2A_1$ or $^2\Sigma$ symmetry results. If the p_y is occupied, a fairly flat surface ($^2B_1$ or $^2\Pi$) is anticipated. *Ab initio* calculations on the carbon and silicon systems (Liskow *et al.* 1974, Pearson and Roueff 1976, Galloy and Lorquet 1978,

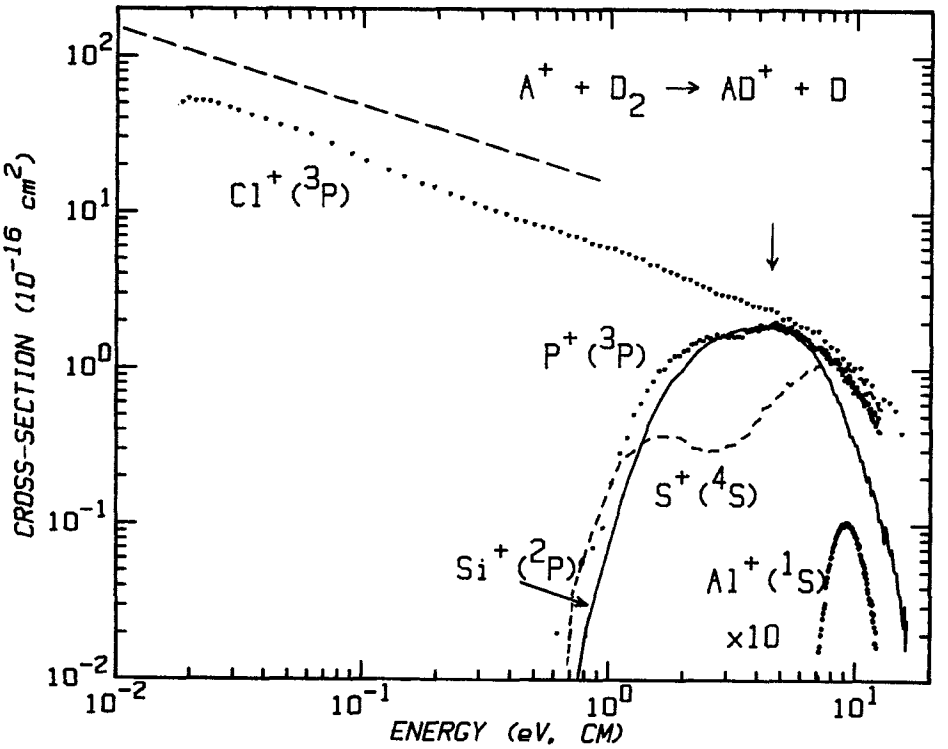

Figure 6. Cross-sections for reaction (1) (with D_2) for $A^+ = Al^+(^1S)$, $Si^+(^2P)$, $P^+(^3P)$, $S^+(^4S)$, and $Cl^+(^3P)$ as a function of kinetic energy in the centre-of-mass frame. The dashed line is σ_{LGS}, calculated by using equation (2). The arrow marks the bond energy of D_2 at 4·6 eV.

Bauschlicher and Shavitt 1980, Sakai *et al.* 1981, Jaquet and Staemmler 1982, Hirst and Guest 1986) verify these ideas and show that the $^2B_1$ surface is repulsive at short internuclear distances. These calculations further show that the attractive $^2B_2$ surface crosses with a $^2A_1$ surface (evolving from $A(^1D) + H_2^+(^2\Sigma)$ reactants) which leads to the potential well of ground state AH_2^+. This crossing is avoided in C_s symmetry, the effective symmetry for all collisions experimentally. The final result is that only one of the three doublet surfaces evolving from $A^+(^2P) + H_2(^1\Sigma_g^+)$ leads to ground state products, $AH^+(^1\Sigma) + H(^2S)$, for collisions in all symmetries (Ervin and Armentrout 1986b, Herbst and Knudson 1981).

9.1. *Carbon*

Reaction (1) with $A^+ = C^+(^2P)$ is probably the best studied endothermic ion–molecule reaction. The 0 K endothermicity of 0·398 ± 0·003 eV is known extremely well from spectroscopic data. Early scattering studies (Iden *et al.* 1971, Mahan and Sloane 1973) established that the reaction proceeds via an intermediate which lives for about one rotational period throughout the low-kinetic-energy region below 4 eV. Early experiments (Maier 1967, Lindemann *et al.* 1972) also examined the kinetic-energy dependence for this reaction but were plagued by uncertainties in the absolute energy scale. As a consequence, the dependence of the absolute cross-section on kinetic energy was not well characterized until recently (Ervin and Armentrout 1984, 1986a, Gerlich *et al.* 1987).

The cross-section measured in our laboratory for room temperature H_2 is shown in figure 4. The reaction is clearly endothermic with an extended plateau followed by a decline beginning at $D^0(H_2)$, a result of process (6). The apparent threshold is substantially lower than the known endothermicity, a result of the thermal motion of the H_2 reactant gas (Doppler broadening). This is shown more clearly in figure 7, where the crossed beam results of Gerlich *et al.* (1987) are also shown. The true threshold behaviour is an excitation function which rises steeply from the thermodynamic threshold and can be modelled using several forms of equation (5) (Ervin and Armentrout 1986a) or less constrained functions (Gerlich *et al.* 1987). While equation (3) fails to reproduce this excitation function, a similar function, $n \approx 0{\cdot}7$ and $m = 1{\cdot}0$, works well. This implies, not unreasonably, that the centrifugal barrier in the exit channel is a dominant constraint in this reaction. This analysis shows unequivocally that there is no activation barrier in excess of the endothermicity for reaction of C^+ with H_2 and that the rotational energy of H_2 is available for reaction.

As noted above, phase-space theory (PST) provides another approach to analysing the kinetic-energy dependence of ion–molecule reactions. Indeed, early tests of PST found it to describe the major features of the $C^+ + H_2$ system quite well (Truhlar 1969, Herbst and Knudson 1981). Comparisons with the recent data (Ervin and Armentrout

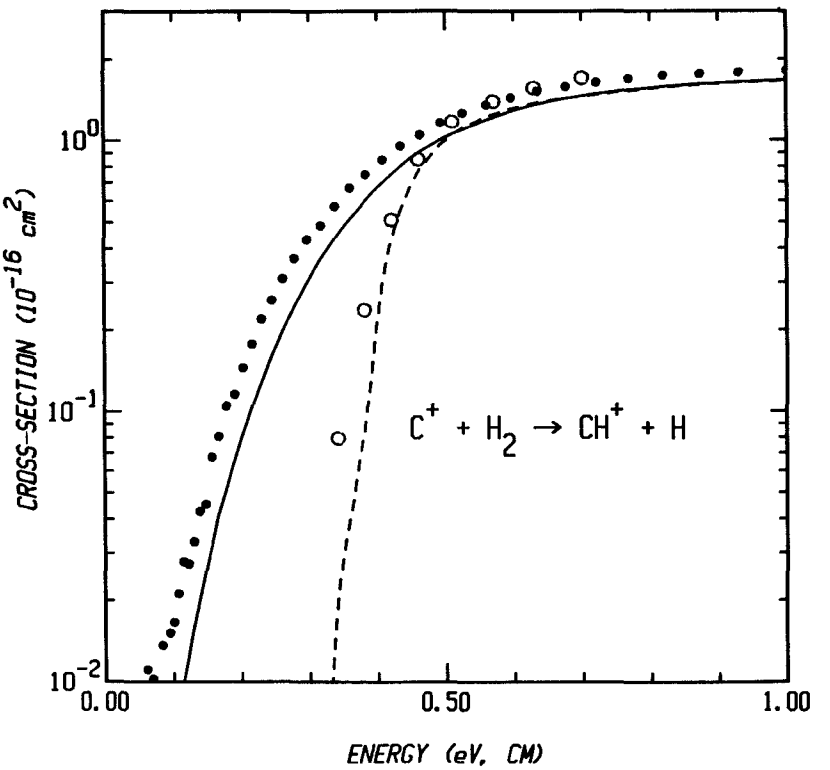

Figure 7. Cross-sections for reaction (1) for $A^+ = C^+(^2P)$ as a function of kinetic energy in the centre-of-mass frame. Experimental results are shown for H_2 at 305 K (closed circles) and in a crossed beam (open circles, results from Gerlich *et al.* (1987)). The dashed line shows a phase space theory calculation, and the full line shows this result convoluted with the experimental energy distribution appropriate for H_2 at 305 K.

1986b, Gerlich *et al.* 1987) find that PST with *no adjustable parameters* describes the shape of the cross-section and its absolute magnitude within about 20% of the experimental results (which have a $\pm 20\%$ uncertainty). This agreement, shown in figure 7, is sufficiently good that it is surprising that a statistical theory reproduces the behaviour of an atom–diatom reaction at elevated energies as well as it does here. This agreement has been attributed to the very deep (4·3 eV) potential well corresponding to the CH_2^+ intermediate.

The input parameters to the PST calculation include the molecular parameters for reactants and products, all of which are well known, and the electronic degeneracies of the reactants and products. The agreement between PST and the data is obtained only when a third of the reactant $C^+ + H_2$ surfaces are presumed to lead to products. This factor emerges from the molecular-orbital analysis discussed above and corresponds to the $^2B_2$ surface being the only reactive one. Note that this also implies that reactants which find themselves on the repulsive $^2A_1$ and $^2B_1$ surfaces do not appear to be able to transfer efficiently to the reactive surface (i.e. there are no large non-adiabatic effects in this system). This observation suggests that as the C^+ and H_2 approach on one of the three surfaces, they become locked onto it with something close to a random probability (although the details of this should depend on the population of the $^2P_{3/2}$ and $^2P_{1/2}$ spin–orbit levels of C^+). (See Gerlich *et al.* (1987) for a more complete discussion of this.) Apparently, non-adiabatic effects which would allow reactants on one of the repulsive surfaces to relax to the attractive surface are inefficient.

The most recent advances concerning this reaction have been the studies of Gerlich *et al.* (1987) which use a crossed beam of *ortho*- and *para*-H_2. This beautifully detailed work demonstrates conclusively that phase-space theory can predict the detailed rotational energy dependence of reaction (1) if one conserves nuclear spin during reaction.

In reaction with HD, formation of CD^+ is favoured over that of CH^+ by a factor of about 1·4 from threshold until the onset of product dissociation (Ervin and Armentrout 1986a). Part of this is attributable to the fact that CD^+ has a lower zero point energy and therefore a lower threshold by 45 meV. Otherwise this isotope ratio is qualitatively comparable to the statistical prediction discussed above, a result consistent with the deep CH_2^+ well and resultant long-lived intermediate. However, neither the simple theory nor PST quantitatively described the branching ratio between formation of CH^+ and CD^+ (Ervin and Armentrout 1986b). This is an indication that, not unexpectedly, dynamics does play a role in this system. As such, this is an avenue for continued exploration.

9.2. *Silicon*

As noted above, one of the main reasons for the near-statistical behaviour of the $C^+ + H_2$ system is believed to be the deep potential well of CH_2^+, 4·3 eV, coupled with the relatively low endothermicity, 0·4 eV. To test whether these features are indeed requirements for such behaviour, we have examined the isovalent reaction with silicon, $A^+ = Si^+(^2P)$ (Elkind and Armentrout 1984). Like $C^+(^2P)$, $Si^+(^2P)$ should easily insert into H_2 on one of three doublet surfaces without an activation barrier. Unlike $C^+ + H_2$, the Si^+ reaction is endothermic by $1{\cdot}26 \pm 0{\cdot}03$ eV (Elkind and Armentrout 1984) and proceeds via a SiH_2^+ potential well which is only $0{\cdot}83 \pm 0{\cdot}07$ eV deep (Boo and Armentrout 1987).

The experimental results (Elkind and Armentrout 1984) for $Si^+ + H_2$ are shown in figure 6. Clearly, the endothermicity of this reaction is greater than that for C^+

(figure 4). The peak in the cross-section again correlates with $D^0(H_2)$. The cross-section behaviour again cannot be represented by equation (3) but is reproduced extremely well by using equation (5) with $n=m=1$ and $E_0=1{\cdot}245\pm0{\cdot}036$ eV. This clearly establishes that the reaction proceeds without an activation barrier in excess of the endothermicity. It is also a nice demonstration that accurate thermochemical data can be derived from beam studies of endothermic reactions.

In unpublished work, we have calculated the result for phase-space theory again with no adjustable parameters and with only one third of the reactant surfaces active. The agreement between PST and the data is excellent both with regards to absolute magnitude and dependence on kinetic energy. The almost-statistical behaviour of this reaction is further substantiated by the reaction of Si^+ with HD. The branching ratio between SiH^+ and SiD^+ is very close to 1:1 throughout the threshold region.

The observation that both $C^+ + H_2$ and $Si^+ + H_2$ behave 'statistically' (although not without dynamic effects) indicates that vibrational periods are probably quite sufficient for extensive energy randomization in the transiently formed triatomic intermediates. A very deep potential well is not required nor must the intermediates be 'long-lived' in the sense of isotropic distributions observed in differential cross-sections. This behaviour is also a reflection that total cross-section measurements such as these involve substantial averaging of molecular orientations and impact parameters which probably serve to 'wash out' dynamic behaviour.

9.3. *Germanium and tin*

While no studies of reaction (1) with $A^+ = Ge^+(^2P)$ or $Sn^+(^2P)$ have been published, we have studied these reactions and those with HD (J. L. Elkind, K. M. Ervin and P. B. Armentrout 1986, unpublished work) and found that they behave comparably to those of $C^+(^2P)$ and $Si^+(^2P)$. Analyses of the thresholds for these reactions provide preliminary values of $D^0(Ge^+\text{–}H)\approx 2{\cdot}9$ eV and $D^0(Sn^+\text{–}H)\approx 2{\cdot}2$ eV, somewhat weaker than $D^0(Si^+\text{–}H)=3{\cdot}23$ eV. Phase-space-theory calculations cannot be performed since the molecular constants for GeH^+ and SnH^+ are unknown.

10. Group 15: nitrogen and phosphorus

The group 15 elemental ions have ^3P ground states with atomic orbital occupations of $(ns)^2(np)^2$ such that there is one empty p orbital. In both C_{2v} and $C_{\infty v}$ symmetries, the most favourable geometry is to have the p_z orbital empty. This leads to an attractive surface having $^3A_2$ or $^3\Sigma^-$ symmetry. Occupation of the p_z orbital leads to repulsive surfaces of $^3B_2$ or $^3\Pi$ symmetry for an empty p_y and $^3B_1$ or $^3\Pi$ symmetry for an empty p_x. This was first discussed for the N^+ reaction by Mahan and co-workers (see for example Hansen *et al.* (1980)) and has been verified by *ab initio* calculations (Gittins and Hirst 1975, Bender *et al.* 1977). The final result is that, like the group 14 ions, only one of the three triplet surfaces which evolve from $A^+(^3P)+H_2(^1\Sigma_g^+)$ is attractive in the entrance channel and eventually leads to products.

10.1. *Nitrogen*

The cross-section for reaction (1) with $A^+ = N^+(^3P)$, the ground state, is shown in figure 4. This cross-section parallels σ_{LGS}, equation (2), but its magnitude is only $\sim\frac{1}{3}$, consistent with the molecular-orbital ideas discussed above. A more detailed statistical model of Gerlich (1989b) suggests that the data are best represented by an electronic factor of $\sim\frac{1}{2}$, which suggests that there may be some (but not extensive) non-adiabatic

coupling between the two non-reactive surfaces and the reactive one. At higher energies, the cross-section declines sharply near the energy onset for product dissociation in process (6). Scattering studies (Hansen *et al.* 1980) show that the reaction intermediate is long-lived at low interaction energies, consistent with formation of a strongly bound NH_2^+ intermediate. This could be the $^3B_1$ ground state accessed via a crossing with the reactive $^3A_2$ surface (which is avoided in C_s symmetry). However, trajectory calculations by González *et al.* (1986, 1989b) suggest that the well corresponding to $NH_2^+(^3A_2)$ could also play a more active role in the reaction dynamics.

While the cross-section shown in figure 4 appears to be a classic example of an exothermic ion–molecule reaction with no barrier, it has long been known that reaction (1) for N^+ is near-thermoneutral, although, until 1985, it was not known whether it was actually exothermic or endothermic. A flurry of recent activity (Luine and Dunn 1985, Marquette *et al.* 1985, 1988, Adams and Smith 1985, Barlow *et al.* 1986, Ervin and Armentrout 1987a, Gerlich 1989b) has firmly established that this reaction is slightly endothermic. The most recent experiments (Marquette *et al.* 1988) and theoretical interpretation (Gerlich 1989b) have reached a consensus that reaction (1) with $N^+(^3P_0)$ is endothermic by 18 ± 12 meV at 0 K. This leads to the interesting consequence that differences in rotational energy of the H_2 and differences in zero point energies for H_2 *versus* HD *versus* D_2 lead to large changes in the endothermicity of reaction. The experiments of Marquette *et al.* (1988) show most conclusively that *n*-H_2 is much more reactive than *p*-H_2 due to the population of higher rotational levels. Differences due to zero point energies are clear from the work of Adams and Smith (1985), Ervin and Armentrout (1987a), and Marquette *et al.* (1988). Results from our laboratory, figure 8, exhibit no clear onsets for these reactions due to the distribution of reactant kinetic energies. However, the cross-sections clearly show that the endothermicity of reaction with H_2 (18 meV) is less than that for D_2 (49 meV) and for reaction (7 *a*) (54 meV), but greater than that for reaction (7 *b*) (6 meV).

Despite the intense scrutiny that this reaction has been subjected to, there remain several interesting issues to be resolved before this system is completely characterized. Definitive studies of the relative reactivities of the spin–orbit states of N^+ ($^3P_0 = 0$ meV; $^3P_1 = 6$ meV; $^3P_2 = 16$ meV) have not been performed. The role of the $^4\Sigma^-$ first excited state of the NH^+ product (which lies only 62 meV above the $^2\Pi$ ground state) is not characterized. It would be interesting to probe experimentally the influence of the quadrupole moment of H_2 on the reactivity, particularly at low energies and temperatures, and thus verify Gerlich's (1989b) calculations on this effect.

10.2. *Phosphorus*

Reaction (1) with $A^+ = P^+(^3P)$ contrasts with that for $N^+(^3P)$ because the reaction is endothermic by 1·16 eV (as calculated from data of Berkowitz *et al.* (1986, 1989)). Further, the ground state of the PH_2^+ intermediate is $^1A_1$, and therefore is no longer accessible in a spin-allowed process from ground state reactants. The lowest lying triplet state, the a^3B_1, is 0·7 eV higher in energy, although it is still stable by 1·76 eV compared with $P^+ + H_2$. In the only published work concerning this reaction, Smith *et al.* (1989) report bimolecular and termolecular rate constants for the association reaction to form PH_2^+ at thermal energies. Their failure to observe reaction (1) is consistent with the endothermicity of the reaction.

In our laboratories, we have recently initiated a detailed study of this reaction (J. M. Behm, E. R. Fisher and P. B. Armentrout 1990, work in progress). Preliminary results,

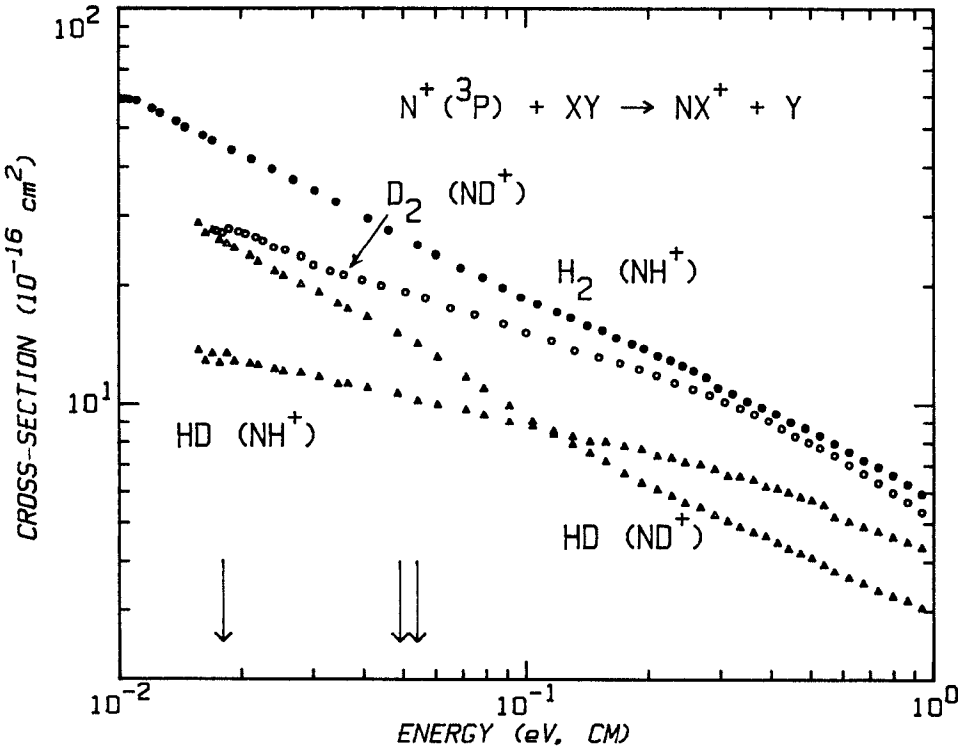

Figure 8. Cross-sections for reaction (1) for $A^+ = N^+(^3P)$ as a function of kinetic energy in the centre-of-mass frame. Results are shown for reaction with H_2 (closed circles), HD (triangles) and D_2 (open circles). Arrows indicate the thresholds for reaction (1) at 18 meV, for reaction with D_2 at 49 meV, and for reaction (7 *a*) at 54 meV.

figure 6, find that the reaction proceeds efficiently once the kinetic energy exceeds the endothermicity (compare the threshold for P^+ to that for Si^+, 0·10 eV higher). Like the Si^+ system, P^+ reacts with HD to form nearly equal amounts of the hydride and deuteride in the threshold region, but unlike Si^+, reaction (7 *b*) is favoured at higher kinetic energies. This isotope effect requires additional study, but may suggest that there is an interesting change in dynamics with kinetic energy. These results also show that excited states of P^+, probably the metastable ^1D and ^1S states, react exothermically and very efficiently with H_2.

11. Group 16: oxygen and sulphur

One of the interesting aspects of reaction (1) for the group 16 ions is that the ground states of the reactant ions are ^4S, but the AH_2^+ intermediates have $^2B_1$ ground states. Thus, access to the deep potential wells corresponding to these intermediates is spin-forbidden from the $A^+(^4S) + H_2(^1\Sigma_g^+)$ reactants. The qualitative character of the single quartet surface evolving from these reactants can be gleaned by examining the occupancy of the A^+ atomic orbitals. This is $(ns)^2(np)^3$ such that the p_x, p_y and p_z are all singly occupied. In C_{2v} symmetry, the potential energy surface is repulsive due to occupation of the p_z orbital. This repulsion is relieved by going to a collinear $C_{\infty v}$ approach. *Ab initio* calculations verify these qualitative ideas for the O^+ reaction (Hirst 1984).

11.1. *Oxygen*

Reaction (1) with $A^+ = O^+(^4S)$ is exothermic by 0·6 eV. The cross-section for this process, shown in figure 4 (Burley *et al.* 1987), can be seen to have three distinct energy regimes. At the lowest energies, $<0{\cdot}25$ eV, the cross-section decreases as $E^{-1/2}$ as predicted by σ_{LGS}, equation (2). Indeed, as shown in figure 4, the agreement between the absolute magnitudes of the experimental data and σ_{LGS} is excellent (better than 5%). While not shown, results for HD and D_2 exhibit identical behaviour (within experimental error limits) and agree equally well with the absolute LGS cross-section. (Contrast this behaviour with the isotopic variation exhibited in figure 8 for N^+.) At the present time, this is certainly one of the best examples of an experimental reaction cross-section which behaves precisely as predicted by equation (2). Note that this agreement means that, at low kinetic energies, the O^+ ion and H_2 molecule apparently have time to orient into the favourable collinear geometry on the single quartet surface. This ability to orient is probably enhanced by the existence of the ion-induced dipole bound O^+–H_2 complex.

At energies above 0·3 eV, the cross-section deviates from the LGS prediction such that the reaction efficiency drops. In the region up to about 5 eV, the cross-section falls approximately as E^{-1} (Burley *et al.* 1987). This is true for all three isotopic systems. The explanation for this behaviour may lie in the fact that this reaction occurs via a direct mechanism, as suggested by the molecular-orbital arguments and demonstrated by scattering studies (Gillen *et al.* 1973). As the kinetic energy is increased, the time available to orient decreases (or equivalently the lifetime of the O^+–H_2 complex decreases) such that the reaction efficiency falls off. This qualitative explanation appears to be consistent with the results of trajectory calculations by González *et al.* (1989a). However, Dateo and Clary (1989) have suggested that the decline is due to competition with vibrational excitation of the H_2 molecule beginning at this energy.

At still higher energies, the cross-section drops more rapidly, $\approx E^{-3}$, due to the dissociation of the product ion in process (6). The observed onset of this decline is somewhat higher than $D^0(H_2)$, about 6 eV, which suggests that some of the energy available to the products is preferentially placed in translation. This is consistent with a direct mechanism for the reaction and with the scattering studies.

Recent work on this reaction has centred on the branching ratio between reactions (7*a*) and (7*b*). Theory has generally had difficulty in reproducing quantitatively the energy dependence of this branching ratio for any atomic ion. Dateo and Clary (1989) have recently found that a rotationally adiabatic theory (Clary 1984) can reproduce this branching ratio fairly accurately for kinetic energies below 0·3 eV. They further predict that this ratio should increase (in favour of OH^+ production) as the rotational energy of the H_2 molecule is reduced. Recent studies in our laboratory for H_2 cooled to ~ 100 K (Sunderlin and Armentrout 1990) verify this prediction and yield a result in reasonable quantitative agreement with the theory. It will be interesting to see whether further applications of this theoretical approach enjoy similar success for reaction (7) with other atomic ions.

11.2. *Sulphur*

While no studies of reaction (1) where $A^+ = S^+(^4S)$ have been reported, the potential energy surface for this reaction has been investigated theoretically (Hirsch and Bruna 1980) due to the interest in state-specific fragmentation of photo-ionized H_2S (Fiquet-Fayard and Guyon 1966, Eland 1979). The reaction is endothermic by about 0·9 eV, and the calculations indicate that the quartet surface is quite repulsive. Recent work in

our laboratories (Stowe *et al.* 1990) finds that $S^+(^4S)$ reacts at the thermodynamic threshold with a small cross-section, and then exhibits a large increase at energies beginning about 2·5 eV and reaching a maximum at about 8 eV, well above $D^0(H_2)$. Reaction with D_2 (figure 6) shows the same behaviour. For reaction with HD, the cross-sections for reactions (7*a*) and (7*b*) both rise at about 0·9 eV with comparable magnitudes, but only the SD^+ product increases at higher energies, beginning at about 1·5 eV and peaking at 6 eV. Thus the low-energy cross-section is behaving statistically while the high-energy feature shows impulsive behaviour.

A detailed account of this study is in preparation, but briefly, we believe that the reactivity observed at the thermodynamic threshold is occurring via a spin-forbidden curve crossing between the $^4A''$ surface evolving from ground state reactants and a $^2A''$ surface which leads to the strongly bound $H_2S^+(X^2B_1)$ ground state intermediate. This is consistent with the statistical behaviour of the low-energy feature. At higher energies, reaction can occur along the repulsive quartet surface in a spin-allowed process. This explains why this feature is larger than the lower-energy feature and why the dynamics exhibit impulsive behaviour. The data is interpreted to yield a barrier of $\sim 1{\cdot}5$ eV for reaction along the quartet surface in what must be a collinear geometry.

12. Group 17: halides

Reaction (1) is exothermic for $A^+ = F^+$ and Cl^+, but endothermic for the other halogens (figure 1). As a consequence, only the chemistry of fluorine and chlorine ions have been studied to date. Because of the $(ns)^2(np)^4$ configuration of the halogen ions, one might expect a similarity with the group 15 elements having $(ns)^2(np)^2$ configurations. However, since there are no unoccupied valence orbitals on the halogen ions, the reaction surfaces should be more repulsive for the group 17 ions than for the group 15 ions. Hence, the halogen ions should probably react via a collinear geometry rather than the perpendicular approach observed for the group 15 ions. (The idea will be discussed more fully for the rare-gas-ion reactions where we have performed more extensive studies.)

12.1. *Fluorine*

The reaction of ground state $F^+(^3P)$ with hydrogen has been carefully studied by Koski and co-workers (Lin *et al.* 1974a, Wendell *et al.* 1975, Jones *et al.* 1977b). Studies in our laboratory confirm the absolute magnitude and energy dependence observed by Lin *et al.* (1974a). The energy dependence of this cross-section follows that of equation (2) fairly closely although the magnitude is about $\sigma_{LGS}/3$. A similar result is obtained by Hamdan *et al.* (1986) at thermal energies. These authors also report a significant contribution from the charge-transfer reaction to form H_2^+ (1·5 times that of the HF^+ channel) but this result is not unequivocal since contributions from excited F^+ states are not characterized and there were problems with secondary reactions. Wendell *et al.* (1975) find that the charge-transfer cross-section is 'significantly smaller' than that for reaction (1). Wendell *et al.* also determine that the reaction proceeds via an intermediate which lives for about a rotational period at the lowest kinetic energies but rapidly turns to a direct reaction at higher energies.

One of the interesting features of this system is that the ionization energy of F atoms, $IE(F) = 17{\cdot}4$ eV, is higher than that of H_2, $IE(H_2) = 15{\cdot}4$ eV and of H, $IE(H) = 13{\cdot}6$ eV. (None of the other elements discussed so far share this property, although it becomes an important consideration for the rare gas atoms, as we shall see.)

One consequence is that the diatomic product no longer decomposes to $A^+ + H$ (reaction (6)) but to $A + H^+$. For fluorine, this dissociation channel opens at 0·7 eV, and indeed the cross-section is observed to decline sharply at about this energy, well before $D^0(H_2)$. Another consequence is that the lowest energy surface in the entrance channel is not $F^+ + H_2$ but $F + H_2^+$. Further, this low-energy surface correlates with $HF + H^+$ rather than $HF^+ + H$. The result, which has been verified by detailed calculations for C_{2v} symmetry (Mahan *et al.* 1978), is that there is no obvious surface that permits reaction (1) to occur for F^+. Mahan *et al.* (1978) conclude that near-$C_{\infty v}$ approaches are probably involved.

12.2. *Chlorine*

The suggestion of Jura (1974) that reaction (1) for $A^+ = Cl^+$ could be important in interstellar chemistry prompted several studies of this reaction at near-thermal energies. Both Smith and Adams (1981) and Kemper and Bowers (1983a) found a weak negative temperature dependence for this reaction. The rate is about half the LGS prediction. Studies in our laboratory, figure 6 (R. H. Schultz and P. B. Armentrout 1990, unpublished work), are in good agreement with these findings. Overall the cross-section behaves quite normally for an exothermic reaction. Scattering measurements by Jones *et al.* (1977a) are complicated by the presence of excited states but show that the reaction is direct for both $Cl^+(^3P)$ and $Cl^+(^1D)$ and that only $HCl^+(^2\Pi)$ is formed. Since $IE(Cl) = 13{\cdot}0$ eV is less than that of H_2 and H, the considerations discussed above for the $F^+ + H_2$ surfaces are not involved here.

13. Group 18: rare gases

Rare gas ions (Rg^+) have the valence electron configuration $(ns)^2(np)^5$. Therefore the ground states are ^2P, like C^+ and Si^+. However, the reactivities of the ^2P states of Rg^+ are quite different from that of carbon and silicon ions. The MO arguments show this readily. As noted above, the less electron density there is in the p_z orbital, the more favourable is the interaction between the ion and H_2 in any geometry. Since Rg^+ must occupy the p_z, it is most favourable to singly occupy this orbital. (We will refer to this as the P_z state of Rg^+. Similarly, if the hole is in the p_x or p_y, these will be the P_x and P_y states.) This leads to a repulsive interaction in C_{2v} symmetry which is relieved in $C_{\infty v}$ symmetry. The P_x and P_y states, both having two electrons in the p_z, are much more repulsive in either geometry. Thus we might expect that the Rg^+ reactions will occur on a third of the available surfaces, with a preference for a collinear geometry. Note that these MO considerations lead naturally to a predicted difference in reactivity between ions with less than half-filled shells (like C^+ and N^+) and those with half-filled shells or more (like O^+, F^+ and Rg^+). The former can proceed via insertion to form strongly bound AH_2^+ intermediates while the latter react in more direct processes.

A more detailed examination of the $Rg^+ + H_2$ surfaces reveals a complication in these systems not encountered in the systems above (except F^+). In the reactions of C^+, N^+ and O^+ with H_2, the reactants in process (1) readily reach the products on a single adiabatic potential-energy surface. For the rare gas ions, a second important surface in the entrance channel is the charge transfer channel, $Rg + H_2^+$. Mahan (1971, 1975) has pointed out that the $RgH^+ + H$ products correlate adiabatically (and diabatically) with $Rg + H_2^+$ and *not* with $Rg^+ + H_2$. This is demonstrated by the observation that the endothermic reaction $He + H_2^+ \rightarrow HeH^+ + H$ is efficient and easily driven by translational and vibrational energy (Chupka and Russell 1968). The coupling between

these two entrance channel surfaces ($Rg^+ + H_2$ and $Rg + H_2^+$) depends strongly on their relative energies as determined by the relative ionization energies of H_2 and the rare gas. Thus the effects of this coupling vary substantially as the rare gas identity changes.

13.1. *Helium and neon*

Reaction (1) is strongly exothermic when $A^+ = He^+(^2S)$ or $Ne^+(^2P)$, by 8·3 and 5·6 eV respectively. Yet in both cases these reactions show no reactivity until very high kinetic energies, 8·1 and 9·8 eV respectively, and then the cross-sections are very small (Ervin and Armentrout 1987b). This is evident in the results for ground state $Ne^+(^2P)$ shown in figure 9. The basic reasons for this non-reactivity have been outlined by Mahan (1971, 1975), Mahan and Winn (1972) and Kuntz and Roach (1972). As for the case of F^+, the interaction of Rg^+ with H_2 occurs on a surface which lies well above that corresponding to $Rg + H_2^+$, and this surface correlates with the desired products, $RgH^+ + H$.

Further insight into these reactions comes from the work of Jones *et al.* (1980) who studied the $He^+(^2S)$ reaction and examined the luminescence from this reaction. Extensive Balmer and Lyman emission was observed with an onset for Lyman α emission coincident with the onset for HeH^+ formation. Thus the process being observed is

$$Rg^+(^2X) + H_2(^1\Sigma_g^+) \rightarrow RgH^+(^1\Sigma) + H^*(2p). \qquad (10)$$

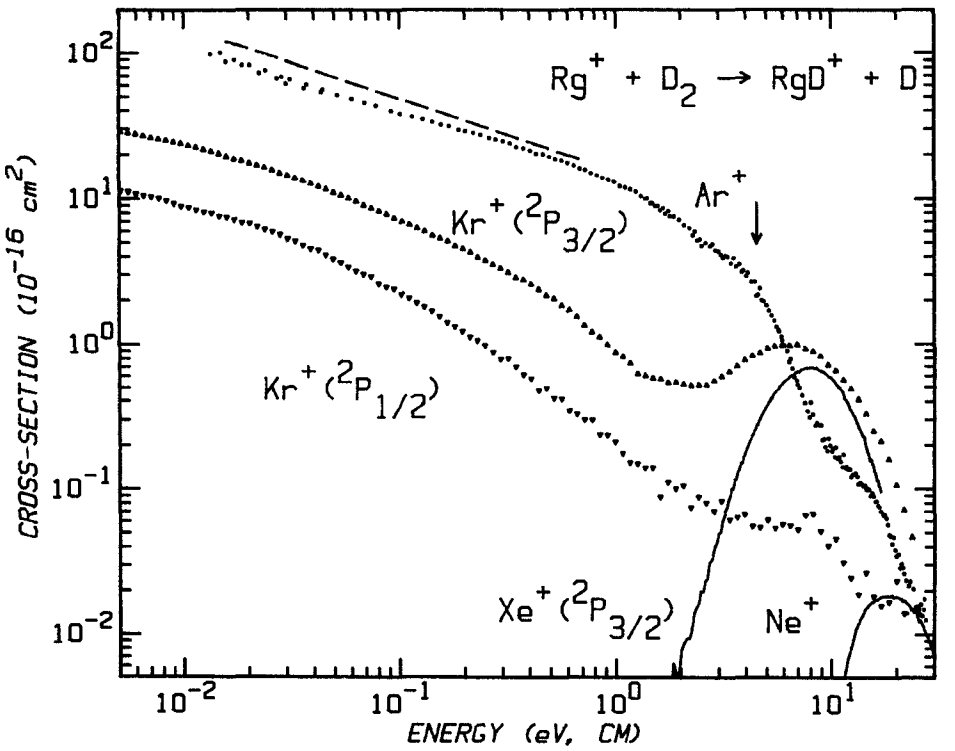

Figure 9. Cross-sections for reaction (1) (with D_2) for $A^+ = Ne^+(^2P)$, $Ar^+(^2P)$, $Kr^+(^2P_{3/2})$, $Kr^+(^2P_{1/2})$, and $Xe^+(^2P_{3/2})$ as a function of kinetic energy in the centre-of-mass frame. The dashed line is σ_{LGS}, calculated by using equation (2). The arrow marks the bond energy of D_2 at 4·6 eV.

Since H(2p) is 10·2 eV above the H(1s) ground state, reaction (10) is endothermic by 1·9 eV for $He^+(^2S)$ and by 4·6 eV for $Ne^+(^2P)$.

While this can explain why He^+ and Ne^+ do not exhibit exothermic behaviour, the observed thresholds of ~ 8 and ~ 10 eV are still well above the calculated endothermicities of reaction (10). Furthermore, the peaks in the cross-sections are also displaced to elevated energies, ~ 20 and ~ 18 eV respectively. Examination of reactions with D_2 and HD help answer why this behaviour is observed. The cross-sections for reaction with D_2 are identical in shape but vary somewhat in size compared to the H_2 reaction cross-sections. The cross-sections for reaction with HD are both similar to that shown for Zn^+ in figure 2. As in this case, this suggests that the reaction is impulsive and that the relevant energy is the 'pairwise' interaction energy discussed above. For the case of Ne^+, the threshold for reaction (10) (or reaction with D_2) is twice the thermodynamic threshold of 4·6 eV (9·2 eV in the CM frame). For reaction with HD to form NeH^+, the pairwise threshold is 13·8 eV ($3 \times 4{\cdot}6$) and to form NeD^+, it is 6·9 eV ($1{\cdot}5 \times 4{\cdot}6$). While the agreement with the data is not quantitative, these energies are in rough agreement with the observed thresholds for all four reactions and appear to capture the essence of the observed variations. For He^+, a similar rough agreement is obtained, although the pairwise threshold is $\sim 1{\cdot}5$ eV, rather than the calculated 1·9 eV threshold for reaction (10). Better agreement is found for the peaks for all products in both systems. These fall at a pairwise energy of about 9 eV: 18 eV in the CM frame for H_2 and D_2, 27 eV for HD, and 13·5 eV for DH. This energy is not obviously related to the thermodynamic onset of a particular dissociation channel (such as $Ne(^1S) + H^+ + H^*(2p)$ at 6·8 eV). These discrepancies are probably related to the details of barriers along the reactive potential energy surfaces, and have been discussed previously (Ervin and Armentrout 1987b).

13.2. *Argon*

Reaction (1) with $A^+ = Ar^+(^2P)$ was long considered to be a classic example of an exothermic reaction which proceeded at the LGS collision limit (Henchman 1972). Our study (Ervin and Armentrout 1985) of this system shows that this belief persisted largely because the cross-section measurements were insufficiently accurate for a definitive evaluation. The cross-section clearly deviates from the behaviour predicted by equation (2) as shown in figure 9 for the case of D_2 (which has an identical cross-section to that for H_2 throughout the energy range examined). The total cross-section for HD is also comparable, except in the region where dissociation of the product becomes important, >4 eV. At the lowest energies, we find that reaction (1) occurs with an efficiency of two-thirds, in agreement with several rate constant measurements (Smith *et al.* 1976, Dotan and Lindinger 1982, Kemper and Bowers 1983b) and with other guided-ion-beam measurements (Teloy and Gerlich 1974). Note that this disagrees with the conclusion of the simple MO treatment that only one-third of the surfaces should be reactive.

As the kinetic energy increases, the reaction efficiency increases to about 90% near 1·0 eV. Above this energy, the cross-section drops as E^{-1} until 4 eV where it falls off rapidly. As in the case of HF^+, the lowest-energy decomposition channel for ArH^+ is to form $Ar + H^+$, beginning at 2·3 eV. While the sharp decline in the cross-section occurs higher than this, this onset corresponds nicely to that predicted by the pairwise energy scheme outlined above (Ervin and Armentrout 1985). The branching ratio between ArH^+ and ArD^+ is nearly unity until dissociation. At the highest energies (beginning

about 8 eV), all three systems exhibit a new feature in the cross-section which we attribute to a process like reaction (10).

Details of the energy-dependent cross-sections can be understood by examining the reaction surfaces. As for the He^+ and Ne^+ systems, it is the $Rg+H_2^+$ surface which diabatically correlates with the $RgH^+ + H$ product surface. Unlike these systems, however, the $Ar^+ + H_2$ surface and the $Ar+H_2^+$ surface have nearly the same energy, such that the diabatic surfaces cross at the bottom of the H_2 well. As Ar^+ and H_2 approach, these two diabatic surfaces readily mix to form two adiabatic surfaces. The lower of these evolves directly to the desired products with no barrier to the overall reaction. No strong inter- or intramolecular isotope effects (such as those observed for He^+ and Ne^+) are observed because the surface interaction occurs at the bottom of the potential well. The decrease in reaction efficiency observed above 1 eV corresponds nicely to a concomitant increase in the charge-transfer cross-section (Ervin and Armentrout 1985). This is a reflection of increasingly diabatic behaviour at these elevated kinetic energies.

The final point of interest is the reaction efficiency at low kinetic energies. In our paper on this system (Ervin and Armentrout 1985), we discussed a number of possible explanations. Since that time, we have conducted experiments, described below, on the reactions of H_2 and $Kr^+(^2P)$ in specific spin–orbit states. These results lead us to believe that spin–orbit effects are responsible for the low-energy behaviour in the Ar^+ system. Similar ideas have also been discussed by Tanaka *et al.* (1981). As shown in the table, the products, $ArH^+(^1\Sigma)+H(^2S)$, have $m_J = \pm\frac{1}{2}$ and $^2A'$ symmetry. The reactant states having this quantum number and symmetry are the $m_J = \pm\frac{1}{2}$ components of $Ar^+(^2P_{3/2})$ and $Ar^+(^2P_{1/2})$. Note that these spin–orbit states are mixtures of the P_x, P_y and P_z states discussed above and that both have some P_z character. Thus the spin–orbit coupling mixes these states such that they both react efficiently. In contrast, the $m_J = \pm\frac{3}{2}$ components of $Ar^+(^2P_{3/2})$ have no P_z character and the wrong symmetry, $^2A''$. They therefore cannot react efficiently at low energies. In a beam with a statistical mixture of $^2P_{3/2}$ and $^2P_{1/2}$ states, this leads to the observed reaction efficiency of $\frac{2}{3}$. As the kinetic energy is increased, mixing of the $^2A''$ and $^2A'$ surfaces can occur leading to an increase in the reaction efficiency. (The nature of this interaction is discussed below.) Further experiments are needed to verify whether this proposed explanation is valid, but it suggests that the $\frac{3}{2}$ state should be less reactive than the $\frac{1}{2}$ state (by a factor of $\sim 50\%$ at thermal energies, decreasing to a factor of $\sim 85\%$ at higher energies). This is qualitatively consistent with the spin–orbit state-specific experiments of Chupka and Russell (1968) and Tanaka *et al.* (1981).

Very recent results (P. Tosi, F. Boldo, F. Eccher, M. Philippi and D. Bassi 1989, private communication), concerning reaction (1) with Ar^+, involve a study with H_2 in a

Asymptotic electronic states in rare gas ion–H_2 systems.

Asymptotic state	J	m_J	$RgHH^+$ state	C_s symmetry
$Rg^+(^2P)+H_2(^1\Sigma_g^+)$	$\frac{3}{2}$	$\pm\frac{1}{2}$	$(\frac{1}{6})^{1/2}(P_x \pm P_y)+(\frac{2}{3})^{1/2}P_z$	$^2A'$
$Rg^+(^2P)+H_2(^1\Sigma_g^+)$	$\frac{3}{2}$	$\pm\frac{3}{2}$	$(\frac{1}{2})^{1/2}(P_x \pm P_y)$	$^2A''$
$Rg^+(^2P)+H_2(^1\Sigma_g^+)$	$\frac{1}{2}$	$\pm\frac{1}{2}$	$(\frac{1}{3})^{1/2}(P_x \pm P_y)-(\frac{1}{3})^{1/2}P_z$	$^2A'$
$Rg(^1S)+H_2^+(^2\Sigma)$	$\frac{1}{2}$	$\pm\frac{1}{2}$		$^2A'$
$RgH^+(^1\Sigma)+H(^2S)$	$\frac{1}{2}$	$\pm\frac{1}{2}$		$^2A'$

molecular beam such that the kinetic energy resolution is much higher than for the gas cell arrangement we use. They find that the cross-section is structured with a sharply decreasing cross-section at the lowest energies, and a new feature which arises at about 0·04 eV. They suggest that the former feature is due to a LGS type of interaction while the latter represents a conversion to direct reaction dynamics. It is possible that these features are also related to the spin–orbit coupling ideas discussed above. This observation shows that this reaction system still holds secrets which more sophisticated experiments can reveal.

13.3. *Krypton*

Reaction (1) with $A^+ = Kr^+(^2P_{3/2})$ is exothermic by $0{\cdot}29 \pm 0{\cdot}06$ eV, while the $^2P_{1/2}$ state reaction is exothermic by 0·96 eV. The spin–orbit splitting of 0·67 eV is sufficiently large that state-specific ion–molecule reactions can be used to produce ion beams of a particular state and the state purity verified by examination of the reaction of Kr^+ with methane (Adams *et al.* 1980). Beams of either spin–orbit state with purities exceeding 95% can be generated in this manner (Ervin and Armentrout 1986c).

The results of this study are shown in figure 9 (Ervin and Armentrout 1986c). Several features are immediately clear from this figure. Reaction with Kr^+ is much less efficient than with Ar^+, and this efficiency is a strong function of the spin–orbit state. The cross-section for the $^2P_{3/2}$ state shows a feature at high energies which is not found in the cross-section for the $^2P_{1/2}$ state. Similar results are also obtained for reaction with HD and H_2 although the total reaction cross-sections show an unusual intermolecular isotope effect such that the relative magnitudes are $\sigma(HD) > \sigma(H_2) > \sigma(D_2)$. The position of the high-energy feature in the $^2P_{3/2}$ cross-section shifts according to the pairwise energy scheme described above.

Many of these observations can be explained by examination of the diabatic and adiabatic surface correlations. Like the other rare-gas-ion systems, formation of products in this reaction involves a crossing from the reactant $Kr^+ + H_2$ diabatic surface to the charge-transfer $Kr + H_2^+$ diabatic surface, although now the $Kr^+ + H_2$ surface lies lower in energy than the $Kr + H_2^+$ surface. As in the Ar^+ system, these diabatic curves mix as the reactants approach to form adiabatic surfaces. This mixing is probably much less efficient than in the case of Ar^+ because the bottom of the reactant well is displaced from the bottom of the charge-transfer well. This delays charge transfer until Kr^+ and H_2 approach more closely than required for $Ar^+ + H_2$. Indeed, this led early workers to hypothesize that a barrier would be observed in the Kr^+ system (Kuntz and Roach 1972), a result which is clearly inconsistent with experiment. However, this surface topology may be manifesting itself in the unusual intermolecular isotope effect, which suggests a dependence on the specific molecular constants of the reactant molecule. The true origins of this effect require further investigation.

The spin–orbit effects discussed in the Ar^+ system are now much clearer. Again it is the $m_J = \pm\frac{1}{2}$ components of $Kr^+(^2P_{3/2})$ and $Kr^+(^2P_{1/2})$ which have the right symmetry to correlate with the charge-transfer species, $Kr + H_2^+$, and the products (see the table). These components are responsible for the low-energy reactivity of the two spin–orbit states. However, only the ground state $Kr^+(^2P_{3/2}, m_J = \pm\frac{1}{2})$ correlates adiabatically and hence it reacts much more efficiently than the $Kr^+(^2P_{1/2}, m_J = \pm\frac{1}{2})$ state. This latter state can react only via non-adiabatic transitions to the $Kr^+(^2P_{3/2}, m_J = \pm\frac{1}{2}) + H_2$ reactive surface. Note that these same non-adiabatic transitions are apparently quite efficient in the $Ar^+ + H_2$ system, presumably because the spin–orbit splitting is much smaller.

Since the high-energy feature in the cross-sections is observed only for reaction of $Kr^+(^2P_{3/2})$, we believe the $m_J = \pm\frac{3}{2}$ components of this state are responsible. As noted above, this surface has the wrong symmetry, $^2A''$, to mix with the reactive $^2A'$ surface such that ordinary non-adiabatic transitions cannot occur. We hypothesize that rotationally non-adiabatic (Coriolis) coupling is the mechanism for this coupling (Ervin and Armentrout 1986c). As noted above, a similar effect probably occurs in the Ar^+ system although at much lower energies.

13.4. *Xenon*

Studies of reaction (1) with $A^+ = Xe^+(^2P)$ have recently been reported for the first time (Ervin and Armentrout 1989). The reaction is endothermic by 0·84 eV for the $^2P_{3/2}$ ground spin–orbit state but exothermic by 0·46 eV for the $^2P_{1/2}$ excited state. This system differs from the other rare gas systems in that the $Xe^+ + H_2$ reactants correlate diabatically with the products. No crossing to the charge-transfer surface is required. Otherwise the adiabatic correlations are the same as those for Kr^+ and Ar^+. Only the $m_J = \pm\frac{1}{2}$ components of the $^2P_{3/2}$ state correlate adiabatically with products.

As in the case of Kr^+, the large spin–orbit splitting (1·3 eV for Xe^+) enable beams of specific spin–orbit states to be produced. Figure 9 shows the results for the $^2P_{3/2}$ state of Xe^+. Despite being exothermic, no reaction due to $Xe^+(^2P_{1/2})$ could definitively be found either at low or high kinetic energies. Presumably the non-adiabatic coupling from this state to $Xe^+(^2P_{3/2}, m_J = \pm\frac{1}{2})$ is much more inefficient than in the Ar^+ and Kr^+ systems due to the larger spin–orbit splitting.

The threshold for reaction of $Xe^+(^2P_{3/2})$ is close to the thermodynamic value but the cross-section rises slowly, suggesting a somewhat repulsive surface (like that for Zn^+). Examination of the HD reaction confirms this by showing thresholds and cross-section maxima which vary in accord with the pairwise energy scheme. While this is the dominant mode of reaction, inefficient reactivity at the thermodynamic threshold is also observed. This weaker process probably occurs along the favourable collinear approach suggested by the MO considerations; however, this steric constraint must limit the efficiency of reaction immediately above threshold. At higher energies, the impulsive reactivity could arise from non-collinear collisions on the ground state $^2A'$ surface (evolving from $Xe^+(^2P_{3/2}, m_J = \pm\frac{1}{2}) + H_2$) or from non-adiabatic transitions from the $^2A''$ surface (evolving from $Xe^+(^2P_{3/2}, m_J = \pm\frac{3}{2}) + H_2$) to the reactive $^2A'$ surface. The latter could be induced by electronic–rotational (Coriolis) coupling as suggested for Kr^+. Indeed the energetics and magnitudes of the $Xe^+(^2P_{3/2})$ cross-sections are similar to the high-energy features in the $Kr^+(^2P_{3/2})$ cross-sections (figure 9).

14. Summary

To a large extent, the periodic variations in reaction (1) which are observed in figures 4, 6 and 9 can be understood by using fairly simple ideas. In some cases, $S^+(^4S)$ and Rg^+ for example, a more detailed understanding of the potential-energy surfaces is clearly needed to explain even the qualitative aspects of the observed reaction cross-sections. While many of these systems are characterized fairly well, there remain many avenues for continued work on reaction (1) which several laboratories are already pursuing and which should be very revealing. An understanding of the intramolecular isotope effects observed in reactions (7 *a*) and (7 *b*) is still at a rudimentary level. The enhanced energy resolution provided by crossed beams of H_2 should yield interesting

new details for the kinetic-energy dependence of reaction (1). Studies which determine the absolute yields of excited-state product formation are needed in many of these systems. Detailed studies of the reactions of state-specific spin–orbit levels for elements other than the rare gases (C^+ and N^+, in particular) would be very useful in elucidating non-adiabatic effects. Finally, studies of other elements not presently included in figure 1 should continue to provide fundamental insight into the periodic trends of chemistry.

Acknowledgments

The work described in this article would not have been possible without the dedication, insight and hard work of my co-workers. Dr Kent M. Ervin and Dr Jerry L. Elkind, in particular, performed most of the experiments described here. The author gratefully acknowledges the continuing support of this work by the National Science Foundation, and also support from the Alfred P. Sloan Foundation, the Camille and Henry Dreyfus Foundation, and the NSF Presidential Young Investigator Program.

References

ADAMS, N. G., and SMITH, D., 1985, *Chem. Phys. Lett.*, **117**, 67.
ADAMS, N. G., SMITH, D., and ALGE, E., 1980, *J. Phys.* B, **13**, 3235.
ADAMS, N. G., SMITH, D., and MILLAR, T. J., 1984, *Mon. Not. R. Astron. Soc.*, **211**, 857.
ARISTOV, N., and ARMENTROUT, P. B., 1986, *J. Am. chem. Soc.*, **108**, 1806.
ARMENTROUT, P. B., 1987, *Structure/Reactivity and Thermochemistry of Ions*, edited by P. Ausloos and S. G. Lias (Dordrecht: D. Reidel), p. 97; 1988, *Comments atomic molec. Phys.*, **22**, 133; 1989, *Gas Phase Inorganic Chemistry*, edited by D. H. Russel (New York: Plenum), p. 1; 1990, *Selective Hydrocarbon Activation*, edited by J. A. Davies and P. L. Watson (New York: VCH) (in the press).
ARMENTROUT, P. B., and BEAUCHAMP, J. L., 1980a, *Chem. Phys.*, **48**, 315; 1980b, *Ibid.*, **50**, 37; 1980c, *J. Am. chem. Soc.*, **102**, 1736; 1981, *Ibid.*, **103**, 784; 1989, *Accts chem. Res.*, **22**, 315.
ARMENTROUT, P. B., and GEORGIADIS, R., 1988, *Polyhedron*, **7**, 1573.
ARMENTROUT, P. B., HODGES, R. V., and BEAUCHAMP, J. L., 1977a, *J. chem. Phys.*, **66**, 4683; 1977b, *J. Am. chem. Soc.*, **99**, 3162.
BARLOW, S. E., LUINE, J. A., and DUNN, G. H., 1986, *Int. J. Mass Spectrom. Ion Processes*, **74**, 97.
BAUSCHLICHER, C. W., and SHAVITT, I., 1980, *Chem. Phys. Lett.*, **75**, 62.
BENDER, C. F., MEADOWS, J. H., and SCHAEFER, H. F., 1977, *Faraday Discuss. chem. Soc.*, **62**, 59.
BERKOWITZ, J., and CHO, H., 1989, *J. chem. Phys.*, **90**, 1.
BERKOWITZ, J., CURTISS, L. A., GIBSON, S. T., GREENE, J. P., HILLHOUSE, G. L., and POPLE, J. A., 1986, *J. chem. Phys.*, **84**, 375.
BOO, B. H., and ARMENTROUT, P. B., 1987, *J. Am. chem. Soc.*, **109**, 3549.
BURLEY, J. D., ERVIN, K. M., and ARMENTROUT, P. B., 1987, *Int. J. Mass Spectrom. Ion Processes*, **80**, 153.
CHANTRY, P. J., 1971, *J. chem. Phys.*, **55**, 2746.
CHUPKA, W. A., and RUSSELL, M. E., 1968, *J. chem. Phys.*, **49**, 5426.
CLARY, D. C., 1984, *Molec. Phys.*, **53**, 3.
COOPER, D. L., GERRATT, J., and RAIMONDI, M., 1986, *Chem. Phys. Lett.*, **127**, 600.
DALY, N. R., 1959, *Rev. Scient. Instrum.*, **31**, 264.
DATEO, C. E., and CLARY, D. C., 1989, *J. chem. Soc. Faraday Trans. II*, **85**, 1685.
DIMPFL, W. L., and MAHAN, B. H., 1974, *J. chem. Phys.*, **60**, 3238.
DOTAN, I., and LINDINGER, W., 1982, *J. chem. Phys.*, **76**, 4972.
ELAND, J. H. D., 1979, *Int. J. Mass Spectrom. Ion Phys.*, **31**, 161.
ELKIND, J. L., and ARMENTROUT, P. B., 1984, *J. phys. Chem.*, **88**, 5454; 1985, *Ibid.*, **89**, 5626; 1986a, *J. chem. Phys.*, **84**, 4862; 1986b, *Inorg. Chem.*, **25**, 1078; 1986c, *J. Am. chem. Soc.*, **108**, 2765; 1986d, *J. phys. Chem.*, **90**, 5736; 1986e, *Ibid.*, **90**, 6576; 1987a, *J. chem. Phys.*, **86**, 1868; 1987b, *J. phys. Chem.*, **91**, 2037; 1988, *Int. J. Mass Spectrom. Ion Processes*, **83**, 259.
ELKIND, J. L., SUNDERLIN, L. S., and ARMENTROUT, P. B., 1989, *J. phys. Chem.*, **93**, 3151.

ERVIN, K. M., and ARMENTROUT, P. B., 1984, *J. chem. Phys.*, **80,** 2978; 1985, *Ibid.*, **83,** 166; 1986a, *Ibid.*, **84,** 6738; 1986b, *Ibid.*, **84,** 6750; 1986c, *Ibid.*, **85,** 6380; 1987a, *Ibid.*, **86,** 1659; 1987b, *Ibid.*, **86,** 6240; 1989, *Ibid.*, **90,** 118.
FIQUET-FAYARD, F., and GUYON, P. M., 1966, *Molec. Phys.*, **11,** 17.
FRIEDRICH, B., and HERMAN, Z., 1982, *Chem. Phys.*, **69,** 433.
GALLOY, C., and LORQUET, J. C., 1978, *Chem. Phys.*, **68,** 479.
GEORGIADIS, R., and ARMENTROUT, P. B., 1988, *J. phys. Chem.*, **92,** 7060.
GERLICH, D., 1989a, *J. chem. Phys.*, **90,** 127; 1989b, *Ibid.*, **90,** 3574.
GERLICH, D., DISCH, R., and SCHERBARTH, S., 1987, *J. chem. Phys.*, **87,** 350.
GILLEN, K. T., MAHAN, B. H., and WINN, J. S., 1973, *Chem. Phys. Lett.*, **22,** 344; 1973, *J. chem. Phys.*, **58,** 5373; 1973, *Ibid.*, **59,** 6380.
GIOUMOUSIS, G., and STEVENSON, D. P., 1958, *J. chem. Phys.*, **29,** 294.
GONZÁLEZ, M., AGUILAR, A., and FERNÁNDEZ, Y., 1986, *Chem. Phys.*, **104,** 57.
GONZÁLEZ, M., AGUILAR, A., and GILIBERT, M., 1989a, *Chem. Phys.*, **131,** 347.
GONZÁLEZ, M., AGUILAR, A., and SAYÓS, R., 1989b, *Chem. Phys.*, **132,** 137.
GITTENS, M. A., and HIRST, D. M., 1975, *Chem. Phys. Lett.*, **35,** 534.
HAMDAN, M., COPP, N. W., BIRKINSHAW, K., JONES, J. D. C., and TWIDDY, N. D., 1986, *Int. J. Mass Spectrom. Ion Processes*, **69,** 191.
HANSEN, S. G., FARRAR, J. M., and MAHAN, B. H., 1980, *J. chem. Phys.*, **73,** 3750.
HENGLEIN, A., 1966, *Ion–Molecule Reactions in the Gas Phase*, edited by P. J. Ausloos (Washington: American Chemical Society), p. 63.
HENCHMAN, M., 1972, *Ion–Molecule Reactions*, Vol. 1, edited by J. L. Franklin (New York: Plenum), p. 101.
HENCHMAN, M. J., ADAMS, N. G., and SMITH, D., 1981, *J. chem. Phys.*, **75,** 1201.
HERBST, E., and KNUDSON, S. K., 1981, *Chem. Phys.*, **55,** 293.
HIRSCH, G., and BRUNA, P. J., 1980, *Int. J. Mass Spectrom. Ion Phys.*, **36,** 37.
HIRSHFELDER, J. O., CURTISS, C. R., and BIRD, R. B., 1954, *Molecular Theory of Gases and Liquids* (New York: Wiley), p. 947.
HIRST, D. M., 1983, *Chem. Phys. Lett.*, **95,** 591; 1984, *J. Phys.* B, **17,** L505; 1987, *J. Chem. Soc. Faraday Trans. II*, **83,** 1615.
HIRST, D. M., and GUEST, M. F., 1986, *Molec. Phys.*, **59,** 141.
IDEN, C. R., LIARDON, R., and KOSKI, W. S., 1971, *J. chem. Phys.*, **54,** 2757.
JAQUET, R., and STAEMMLER, V., 1982, *Chem. Phys.*, **68,** 479.
JONES, C. A., SAUERS, I., KAUFMAN, J. J., and KOSKI, W. S., 1977a, *J. chem. Phys.*, **67,** 3599.
JONES, C. A., WENDELL, K. L., and KOSKI, W. S., 1977b, *J. chem. Phys.*, **67,** 4917.
JONES, E. G., WU, R. L. C., HUGHES, B. M., TIERNAN, T. O., and HOPPER, D. G., 1980, *J. chem. Phys.*, **73,** 5631.
JURA, M., 1974, *Astrophys. J.*, **190,** L33.
KEMPER, P. R., and BOWERS, M. T., 1983a, *Int. J. Mass Spectrom. Ion Phys.*, **51,** 11; 1983b, *Ibid.*, **52,** 1.
KLIMO, V., TINO, J., and URBAN, J., 1986, *Chem. Phys.*, **104,** 207.
KRENOS, J. R., PRESTON, R. K., WOLFGANG, R., and TULLY, J. C., 1974, *J. chem. Phys.*, **60,** 1634.
KUNTZ, P. J., and ROACH, A. C., 1972, *J. chem. Soc. Faraday Trans. II*, **68,** 259.
KUSINOKI, I., and OTTINGER, CH., 1979, *J. chem. Phys.*, **71,** 4227; 1980, *Ibid.*, **73,** 2069; 1982, *Ibid.*, **76,** 1845; 1984, *Ibid.*, **80,** 1872.
LEVINE, R. D., and BERNSTEIN, R. B., 1972, *J. chem. Phys.*, **56,** 281.
LIAS, S. G., BARTMESS, J. E., LIEBMAN, J. F., HOLMES, J. L., LEVIN, R. D., and MALLARD, W. G., 1988, *J. Phys. Chem. Ref. Data*, **17,** Suppl. 1.
LIFSHITZ, C., WU, R. L. C., TIERNAN, T. O., and TERWILLIGER, D. T., 1978, *J. chem. Phys.*, **68,** 247.
LIN, K.-C., COTTER, R. J., and KOSKI, W. S., 1974a, *J. chem. Phys.*, **61,** 905.
LIN, K.-C., WATKINS, H. P., COTTER, R. J., and KOSKI, W. S., 1974b, *J. chem. Phys.*, **60,** 5134.
LINDEMANN, E., FREES, L. E., ROZETT, R. W., and KOSKI, W. S., 1972, *J. chem. Phys.*, **56,** 1003.
LISKOW, D. H., BENDER, C. F., and SCHAEFER, H. F., III, 1974, *J. chem. Phys.*, **61,** 2507.
LUINE, J. A., and DUNN, G. H., 1985, *Astrophys. J.*, **299,** 167.
MAHAN, B. H., 1971, *J. chem. Phys.*, **55,** 1436; 1975, *Accts chem. Res.*, **8,** 55.
MAHAN, B. H., RUSKA, W. E. W., and WINN, J. S., 1976, *J. chem. Phys.*, **65,** 3888.
MAHAN, B. H., SCHAEFER, H. F., III, and UNGEMACH, S. R., 1978, *J. chem. Phys.*, **68,** 781.
MAHAN, B. H., and SLOANE, T. M., 1973, *J. chem. Phys.*, **59,** 5661.

MAHAN, B. H., and WINN, J. S., 1972, *J. chem. Phys.*, **57,** 4321.
MAIER, W. B., 1967, *J. chem. Phys.*, **46,** 4991.
MANDICH, M. L., HALLE, L. F., and BEAUCHAMP, J. L., 1984, *J. Am. chem. Soc.*, **106,** 4403.
MARQUETTE, J. B., ROWE, B. R., DUPEYRAT, G., and ROUEFF, E., 1985, *Astron. Astrophys.*, **147,** 115.
MARQUETTE, J. B., REBRION, C., and ROWE, B. R., 1988, *J. chem. Phys.*, **89,** 2041.
MÜLLER, B., and OTTINGER, CH., 1986a, *J. chem. Phys.*, **85,** 232; 1986b, *Ibid.*, **85,** 243.
OCHS, G., and TELOY, E., 1974, *J. chem. Phys.*, **61,** 4930.
OTTINGER, CH., and REICHMUTH, J., 1981, *J. chem. Phys.*, **74,** 928.
PEARSON, P. K., and ROUEFF, E., 1976, *J. chem. Phys.*, **64,** 1240.
RAIMONDI, M., and GERRATT, J., 1983, *J. chem. Phys.*, **79,** 4339.
ROSMUS, P., and KLEIN, R., 1984, Thesis by R. Klein, Universität Frankfurt.
RUATTA, S. A., HANLEY, L., and ANDERSON, S. L., 1989, *J. chem. Phys.*, **91,** 226.
SAKAI, S., KATO, S., MOROKUMA, K., and KUSONOKI, I., 1981, *J. chem. Phys.*, **75,** 5398.
SCHNEIDER, F., ZÜLICKE, L., POLÁK, R., and VOJTÍK, J., 1984, *Chem. Phys. Lett.*, **105,** 608; 1984b, *Chem. Phys.*, **84,** 217.
SMITH, D., and ADAMS, N. G., 1981, *Mon. Not. R. Astron. Soc.*, **197,** 377.
SMITH, D., MCINTOSH, B. J., and ADAMS, N. G., 1989, *J. chem. Phys.*, **90,** 6213.
SMITH, R. D., SMITH, D. L., and FUTRELL, J. H., 1976, *Int. J. Mass Spectrom. Ion Phys.*, **19,** 395.
SONDERGAARD, N. A., SAUERS, I., JONES, A. C., KAUFMAN, J. J., and KOSKI, W. S., 1979, *J. chem. Phys.*, **71,** 2229.
SONDERGAARD, N. A., SAUERS, I., KAUFMAN, J. J., and KOSKI, W. S., 1982, *J. phys. Chem.*, **86,** 533.
STOWE, G. S., SCHULTZ, R. H., WIGHT, C. A., and ARMENTROUT, P. B., 1990, *Int. J. Mass Spectrom., Ion Processes* (to be published).
SUNDERLIN, L., ARISTOV, N., and ARMENTROUT, P. B., 1987, *J. Am. chem. Soc.*, **109,** 78.
SUNDERLIN, L. S., and ARMENTROUT, P. B., 1988, *J. phys. Chem.*, **92,** 1209; 1990, *Chem. Phys. Lett.*, **167,** 188.
TALROSE, V. L., VINOGRADOV, P. S., and LARIN, I. K., 1979, *Gas Phase Ion Chemistry*, Vol. 1, edited by M. Bowers (New York: Academic), p. 305.
TANAKA, K., DURUP, J., DATO, T., and KOYANO, I., 1981, *J. chem. Phys.*, **74,** 5561.
TELOY, E., and GERLICH, D., 1974, *Chem. Phys.*, **4,** 417.
TRUHLAR, D. G., 1969, *J. chem. Phys.*, **51,** 4617.
VILLIGER, H., HENCHMAN, M. J., and LINDINGER, W., 1982, *J. chem. Phys.*, **76,** 1590.
WATSON, W. D., 1977, *Acc. Chem. Res.*, **10,** 221.
WEBER, M. E., ELKIND, J. L., and ARMENTROUT, P. B., 1986, *J. chem. Phys.*, **84,** 1521.
WENDELL, K., JONES, C. A., KAUFMAN, J. J., and KOSKI, W. S., 1975, *J. chem. Phys.*, **63,** 750.